Summer 2009

Synthesis of surface composites using friction stir processing

Bharat Gattu

Department:

SYNTHESIS OF SURFACE COMPOSITES USING FRICTION STIR PROCESSING

by

BHARAT GATTU

A THESIS

Presented to the Faculty of the Graduate School of the

MISSOURI UNIVERSITY OF SCIENCE AND TECHNOLOGY

In Partial Fulfillment of the Requirements for the Degree

MASTER OF SCIENCE IN MATERIALS SCIENCE AND ENGINEERING

2009

Approved by

Rajiv S. Mishra, Advisor
F. Scott Miller
Lokesh R. Dharani

PUBLICATION THESIS OPTION

This thesis consists of the following two articles that have been prepared for submission for publications as follows:

Page 18-34 are intended for submission to the MATERIALS SCIENCE AND ENGINEERING A.

Page 35-50 are intended for submission to the MATERIALS SCIENCE AND ENGINEERING A.

ABSTRACT

Composite materials have an edge over monolithic materials due to higher strength/stiffness – to – density ratios, improved fatigue and wear resistance and better high temperature properties. Surface composites provide improved tribological properties such as wear resistance, friction coefficient and corrosion resistance. Friction stir processing (FSP) which originated from friction stir welding (FSW – a method for joining aluminum alloys) is a solid state technique to modify the microstructure of the alloys. During FSP the frictional heat generated at the tool – work piece interface plasticizes the material allowing it to flow around the pin. The combined effect of the plastic deformation and the generated heat leads to grain refinement in the alloys.

In the present work, effort has been made to expand the scope of FSP as a novel method for the synthesis of surface composites. Different ways for incorporation of SiC particles into Al1100 alloy were explored and compared with each other. The response of the flow of the powder in the substrate during FSP has been studied for different processing features. The effects of various parameters and methodology on the incorporation and distribution of SiC particles in the nugget, the microstructure and mechanical properties of the composite layer were studied.

ACKNOWLEDGMENTS

I would like to thank my advisor, Dr. Rajiv S. Mishra, for giving me a great opportunity to work in this innovative research area. I am grateful to him for giving me continuous support, guidance and encouragement in this endeavor. His knowledge and patience encouraged me through the journey of my research. I would also like to acknowledge the NSF I/UCRC program for providing the funding and the additional support of Boeing, PNNL, GM and Friction Stir Link.

I am grateful to my committee members, Dr. F. Scott Miller and Dr. Lokesh R. Dharani for their valuable suggestions and input for this work.

I would also like to take this opportunity to extend my sincere thanks to all my present and former colleagues. I am especially grateful to Kumar and Nilesh Kumar for their valuable suggestions and assistance. I am also grateful to Dr. Wang, Dr. Dutta, Saumydeep Jana, Partha De, Jeff Rodelas, Gaurav Bhargava, Yuan Wei, Arun Mohan, Jiye Wang, Gaurav Argade, Neal Ross, Prabhanjana Kalya, Nagarajan Balasubramanian, Marco Garcia and Steve Webb.

This thesis is dedicated to my dearest parents, my brother and my friends (Abhi, Argha, Sagnik and Shashwat) who stood by me, encouraged me to pursue my dreams and expected great things for me.

TABLE OF CONTENTS

LIST OF ILLUSTRATIONS

LIST OF TABLES

1. INTRODUCTION

1.1 COMPOSITE MATERIALS

Composite materials are multiphase materials obtained by the artificial combination of different materials, so as to obtain different properties which the individual materials cannot obtain by themselves [1]. They contain discrete material or phases distributed in a preferred manner. The different phases which constitute the composites are not formed naturally by reactions or phase transformations and are often introduced into the system externally. These materials provide a wide range of properties by the combination of the properties of the individual materials.

This class of advanced engineering materials consists of reinforcement, also termed as fillers, in a continuous material, termed as the matrix. The reinforcement and the matrix individually contribute to the bulk properties of the composite material which are designed according to the application. For example, a carbon fiber composite consists of fillers with at least one of them being carbon fibers and a matrix which can be a polymer, metal, carbon, ceramic or combination of materials. Although carbon fibers are brittle, they are used as reinforcement in a low strength polymer matrix to obtain intermediate mechanical properties due to their high strength and modulus. The higher electrical and thermal conductivity of carbon fibers induces an added functionality while the low thermal expansion coefficient serves to reduce the thermal expansion of the polymer matrix[1].

Composites can be categorized based on type of matrix and the geometry of the reinforcing phase.

1.1.1 Geometry of Reinforcement: Based on the aspect ratio of the reinforcement, which is defined as the ratio of equivalent diameter to the length of the reinforcement, composites are classified into the following categories (Figure 1.1 and Figure 1.2)[2]:

a) Particulate reinforced composites
b) Short fiber/whisker reinforced composites
c) Continuous fiber reinforced composites
d) Sheet reinforced composites

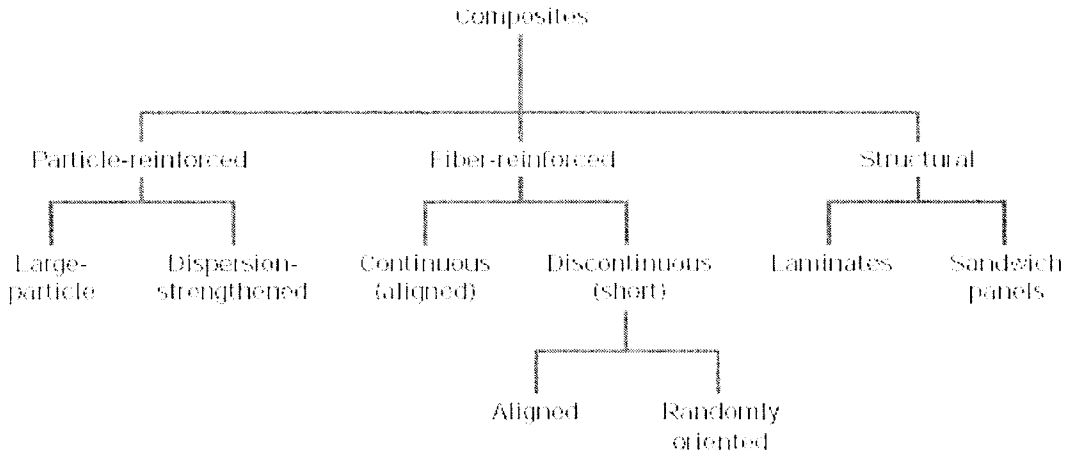

Figure 1.1. Classification of composites based on reinforcement [3].

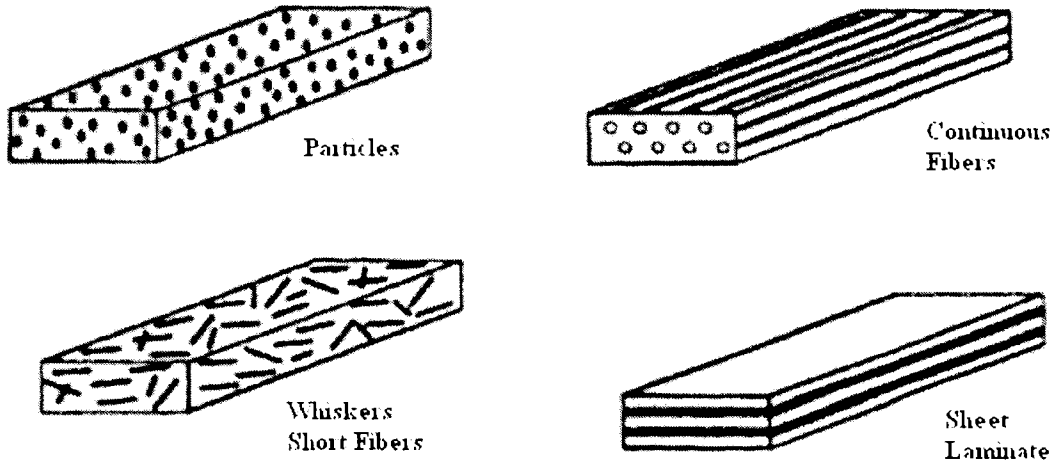

Figure 1.2. Pictorial representation of the composites based on reinforcement[2].

The geometry of the reinforcement determines the stress field around the reinforcement and thus, directly affects the load transfer process in the composite material. Anisotropy is also introduced in the material by obtaining a particular alignment of the filler material. For example, the Young's modulus of a continuous fiber reinforced composite is higher along the axis of the fiber and reaches a minimum normal to it. The fracture mechanism of the composite is influenced by the geometry of the particles and the direction of loading.

1.1.2 Type of Matrix: Based on the type of matrix, composites can be classified as follows[4]:

a) Polymer matrix composite (PMC)
b) Metal matrix composite (MMC)
c) Ceramic matrix composite (CMC)
d) Carbonaceous matrix composite (CCC)
e) Fiber reinforced polymeric composite (FRPC)
f) Particulate – reinforced metal matrix composite (PMMC)

1.1.2.1. Polymer matrix composite (PMC): Polymer matrix composites are easier to fabricate as compared to metal matrix, ceramic matrix or carbon matrix composites, due to low processing temperatures. PMC can be further classified as thermosetting and thermoplastic polymer composites.

Thermosets like epoxy cure irreversibly and are processed at temperatures ranging from room temperature to 200°C. They are associated with cross linking of the polymeric chains. Thermoplastics such as polyimide or polyetheretherketone can be cured reversibly and molded into a different shape when heated to temperatures ranging from 300°C – 400°C. Hence, thermoplastics have higher processing speeds and show more ductility than thermosets. They have gained increased importance with the availability of thermoplastics which can withstand high temperature[1].

Thermoplastics have lower manufacturing costs due to unlimited shelf life, the possibility of reprocessing, low moisture content, weldability and ability of thermal shaping. They provide higher toughness and show higher tolerance to environmental conditions as compared to thermosets; however, suffer due to limited processing techniques, higher processing temperatures, higher viscosities and less developed fiber surface treatment processes.

1.1.2.2. Metal matrix composite (MMC): Metal matrix composites offer major weight savings due to higher strength – to – weight ratio, dimensional stability, elevated temperature properties and higher fatigue life as compared to monolithic metallic alloys and hence, find a major application in aerospace and automotive industries. When compared to PMCs, they are marked by higher strength and stiffness, higher operating temperatures, higher thermal and electrical conductivity, better transverse properties, improved joining characteristics, radiation survivability and no contamination by moisture. Table 1.1 shows a list of different commercial reinforcements used for MMCs.

Table 1.1. List of reinforcements used in MMCs[2]

Continuous Fibers	Al_2O_3, +SiC, B , C, SiC, Si_3N_4, Nb – Ti, Nb_3Sn
Discontinuous Fibers	
a. Whiskers	SiC, TiB_2, Al_2O_3
b. Short fibers	Al_2O_3, SiC, (Al_2O_3+SiO_2), vapor grown carbon
Particles	SiC, Al_2O_3, TiC, B_4C, WC

By adding ceramic particles, the coefficient of thermal expansion of the composite decreases and can be used in applications involving electronic packaging. WC/Co and SiC_p/Al composites find application in wear resistance and are often used as cutting tools, wear drilling inserts and rotors in brakes.

1.1.2.3. Ceramic matrix composite (CMC): Ceramic matrix composites form an attractive class of materials for high temperature applications because of their high oxidation resistance. The reinforcement serves the purpose of increasing the toughness, tensile and flexural strength of the composite and decreases the drying shrinkage in ceramic matrices fabricated from slurries and slips.

The desirable characteristics of CMCs include high-temperature stability, high thermal shock resistance, high hardness, high corrosion resistance, light weight, nonmagnetic and nonconductive properties, and versatility in providing unique engineering solutions. A comparison of the mechanical behavior of continuous fiber reinforced composite to a monolithic ceramic is shown in Figure 1.3.

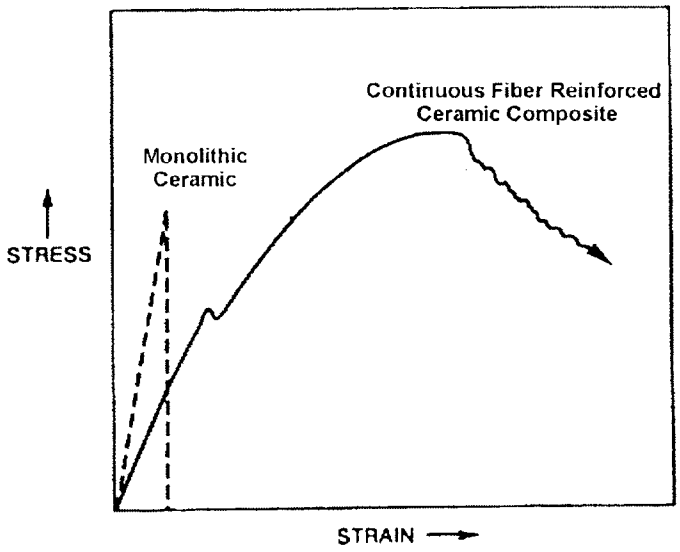

Figure 1.3. Typical comparison of failure modes for monolithic ceramics and continuous fiber reinforced ceramic composites[5].

1.2. SURFACE COMPOSITES

Surface composites are different from other engineered materials such as "bulk composites" and "functionally graded materials" (FGM). Unlike bulk composites, the surface phase in surface composites is present only at the near surface regions and in

contrast to FGM the graded properties of surface composites are achieved by morphological surface modification of the bulk phase[6] (Figure 1.4).

One of the most important features of surface composites is formation of a mechanically and compositionally graded three dimensional interface between the two materials. Due to linear gradation of thermal, mechanical and residual stresses; creation of pseudo diffusion layer between the two materials; higher interfacial area and the mechanical interlocking of the two layers, a high degree of adhesion is expected from the two phases.

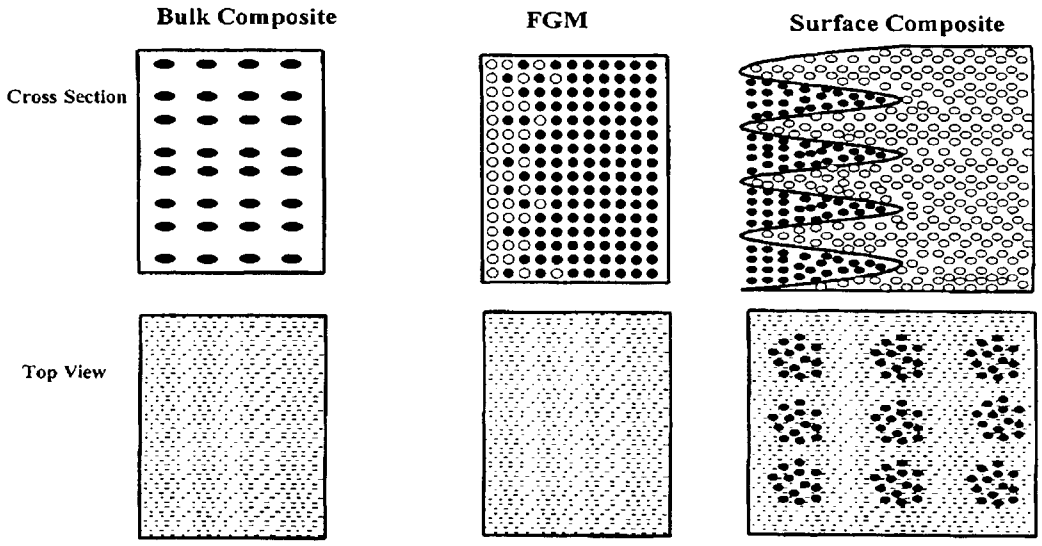

Figure 1.4. Schematic diagram showing the cross section and top view of various engineered materials: (left) bulk composite, (middle) functionally graded material (FGM), and (right) surface composite material[6].

Surface composites provide improved tribological properties of the surface such as the wear resistance and better sliding friction coefficient, to tailor the surface adhesion characteristics towards a particular application (for example, to improve bio compatibility) and induce functionality in the surface. For example, by using high microwave absorptive material, the surface composite can be used for radar applications in stealth technology.

1.3. CONVENTIONAL MANUFACTURING OF SURFACE COMPOSITES

Deuis et al.[7] have mentioned laser cladding[8], thermal spraying[9] and discussed plasma transferred arc (PTA) as methods to deposit MMC onto ferrous and non – ferrous substrates. PTA surfacing is a modification of the plasma arc welding method and emerged from the basic principles of traditional welding surfacing techniques such as oxy – fuel gas welding, gas tungsten arc process, manual metal arc welding and submerged arc welding. The coating consumables are in powder form instead of wire or rod and hence, PTA provides higher deposition rates, a relatively low dilution and broader compositional choice of coatings.

The PTA apparatus (Figure 1.5) consists of a tungsten cathode and a water cooled copper anode with a mechanism for the circulation of argon gas between the two electrodes though the inner annulus. Initially, a high frequency arc is started between the two electrodes, ionizing the argon gas, which provides a current path for a transferred arc and heats the metal substrate creating a weld pool.

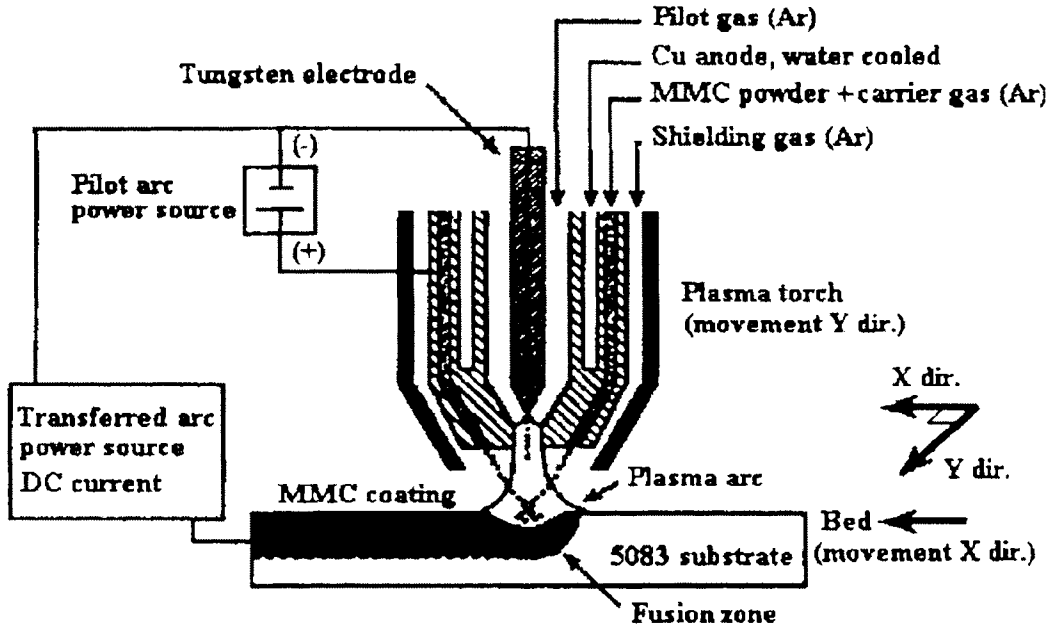

Figure 1.5. Schematic diagram of PTA surfacing process[7].

The powder is transported through the torch such that it intersects the plasma above the substrate and gets introduced into the weld pool which is protected from oxidation by the shielding gas.

Laser melt particle injection process[10-11] (Figure 1.6) is another method for producing the metal matrix composite layer on the top of the substrate. In the laser cladding process, the coating is created by melting the powder, forming a new alloyed layer after the mixture with the substrate materials. However, in laser melt particle injection the melting is limited to a level such that the particle forms a good bond with the substrate at the interface.

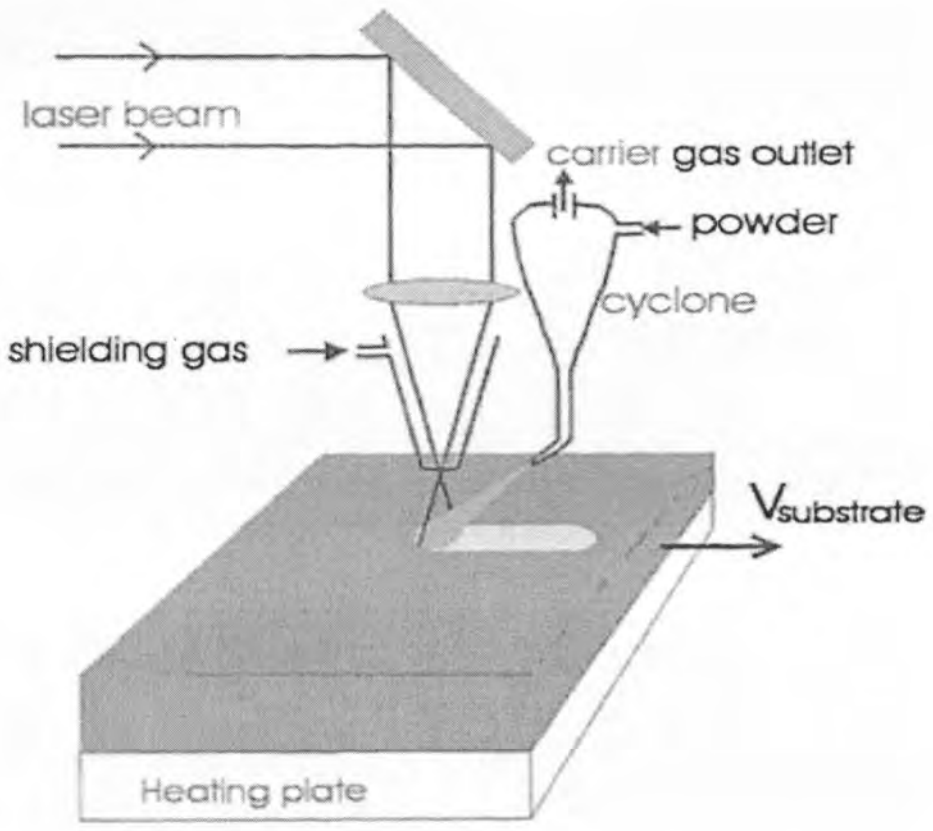

Figure 1.6. Schematic picture of laser melt particle injection process[10].

Due to the high reflectivity of certain substrate surfaces (for example aluminum) either a high energy density of the laser is required for processing or a surface treatment (like sand blasting) is required to reduce the reflectivity of the surface. The process of injection is very sensitive to fluctuations in power density, preheating temperature, powder flow characteristics and hence, has limited scope of operational parameters.

1.4. FRICTION STIR WELDING (FSW)

Friction stir welding[12] (Figure 1.7) is a solid state joining process which was developed at The Welding Institute (TWI), United Kingdom in 1991. In FSW, a rotating non consumable tool is driven into the faying surface of the two weld plates and then traversed along the weld line. The tool, which consists of a pin and shoulder, is specially designed to generate ample heat to soften the material and maximize flow of material. Heat generated due to the friction between the workpiece and the rotating tool along with the severe plastic deformation of the material causes localized heating around the pin. This softens the material and causes movement of material from the front to the back of the pin under the influence of tool rotation and translation, filling up the hole created at the back as tool moves forward.

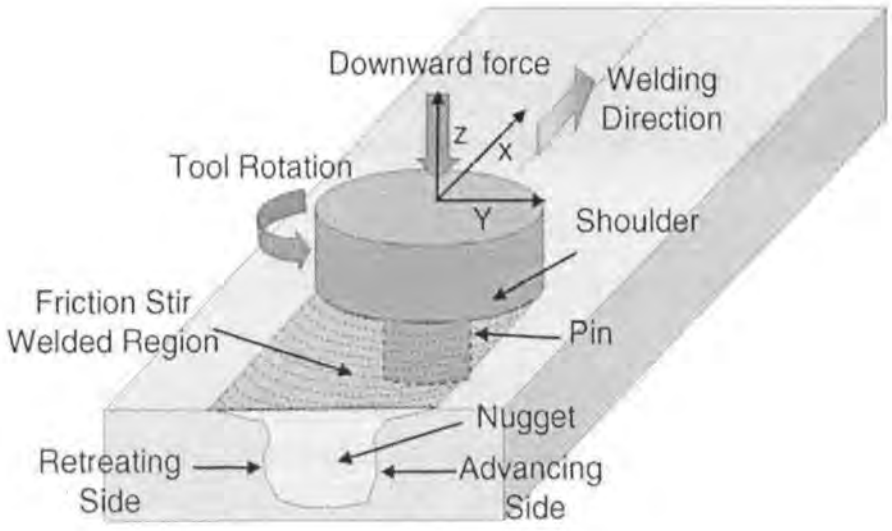

Figure 1.7. Schematic drawing of friction stir welding[13].

The advancing side is defined as one where the tool rotation is same as the tool travel direction while the retreating side is one where the tool rotation is opposite to the tool travel direction. The side of the shoulder which is in contact with the fresh material (or faying surface) is called the leading edge and the one which is in contact with the plastically deformed material (deposited material) is called the trailing edge.

The functions of the tool are as follows:

a. Heating the work piece to plasticize the material.
b. Force the movement of material producing a joint.
c. Contain the material below the shoulder during welding.

The weld zone can be divided into the distinct regions as follows (Figure 1.8):

a. Parent material.
b. Heat affected zone.
c. Thermomechanically affected zone.
d. Weld nugget.

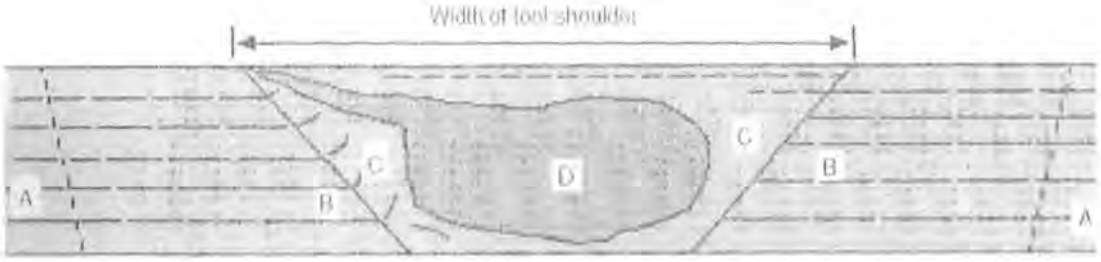

Figure 1.8. Microstructural regions in the transverse cross section of friction stir welded material[12].

The processing parameters that influence the properties of the weld are the speed of rotation of tool (given in revolutions per minute, rpm), the tool travel speed (given in inches per minute, ipm), the plunge depth and the tool travel angle. Using a proper set of parameters, a solid–state joint is achieved without any melting. The advantages of FSW over traditional welding methods are as follows:

a. Provides improved microstructural and mechanical properties without any solidification defects in the weld.

b. Dimensionally stable and environmentally clean process.
c. Lower energy process since no melting is involved.

1.5 FRICTION STIR PROCESSING (FSP)

Friction stir processing is a modification of FSW with the same process features except that it is employed in modifying the properties of the alloys instead of welding two surfaces. FSP can be used as a process to selectively modify the microstructure and change the composition of alloys. It has found wide applications for enhancing superplasticity, improving room temperature formability, casting modification, improving the fatigue properties and corrosion resistance[14-22].

The concepts which enable FSP as a tool to improve the properties of alloys are as follows[12]:

a. Low heat input.
b. Maximum plastic flow of material.
c. Fine grain size in nugget due to plastic deformation.
d. Removal of defects and porosity.
e. Large density of randomly oriented grain boundaries.
f. Mixing of layers mechanically without fusion.

1.6 TOOL DESIGN FOR FSP

The tool design (Figure 1.9) is one of the most important aspects of FSP which directly determines the flow characteristics in the alloy during processing and hence, the properties of the processed material. A proper selection of tool material and features is required to obtain a good quality processed zone and to make sure that the wear and fracture of tool is avoided during FSP.

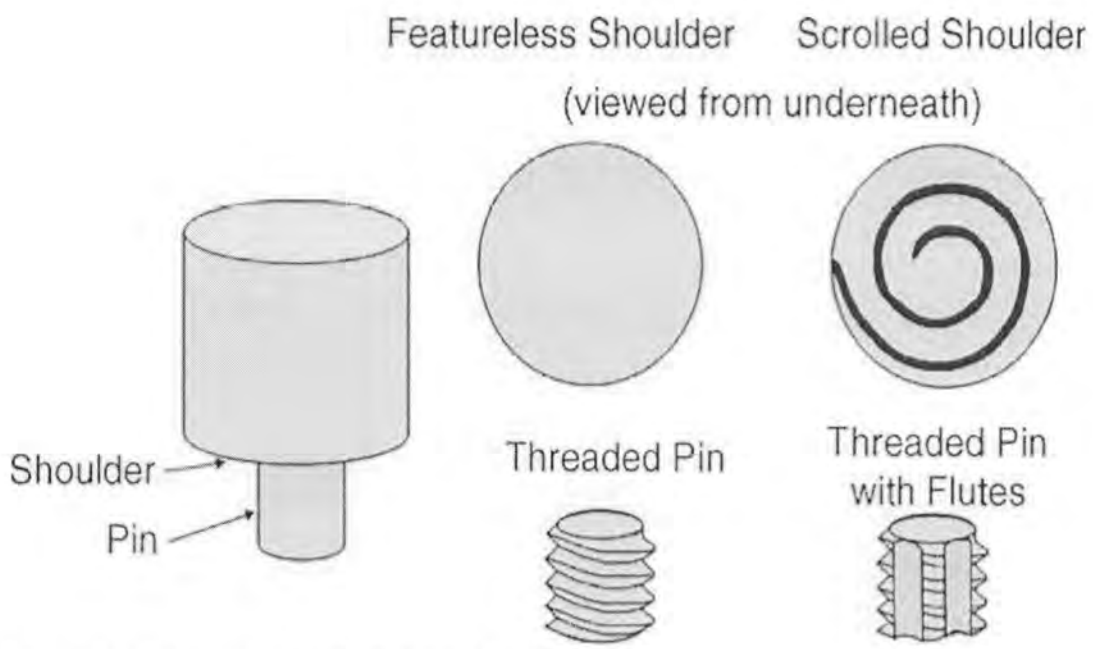

Figure 1.9. Schematic drawing of FSW tool[13].

The tool material selection is guided by the following factors:

a. Ambient and elevated temperature strength.
b. Elevated temperature stability.
c. Reactivity of tool.
d. Fracture toughness.
e. Coefficient of thermal expansion.
f. Machinability and availability.
g. Uniformity in microstructure and density.

Tool steels, WC–Co MP159, nickel alloys, tungsten alloys, polycrystalline cubic boron nitride (PCBN) and tungsten carbide are a few examples of the tool materials which are used in commercial applications.

The tool shoulder is designed to optimize the heat generated and heat flow during the process. It is also required to provide a forging action for the consolidation of the material. The majority of the tools are designed to have a concavity in the shoulder to

contain the material. This acts as a reservoir for the forging action at the rear of the shoulder when new material forces it to flow back as the tool moves forward. The shoulders are also provided with features such as scrolls to guide the material flow from the edge of the shoulder to the pin.

The pin is designed to maximize the heat generation and sub–surface material flow which plays an important role when processing thicker cross sections. Various commercially – used pins include the round–bottom cylindrical pin, flat–bottom cylindrical pin, truncated cone pins, pins with machines flats, whorl pin, MX triflute pin, trivex pin, threadless pin and retractable pin.

1.7 HEAT AND MATERIAL FLOW

The heat distribution around the tool is asymmetric and the dominating source of heat generation is influenced by the processing parameters, the tool features and the thermal conductivities of the material and the backing plate. It is observed that the major heat generation occurs at the shoulder–material interface[23]. The sliding or sticking conditions at the pin–material interface determine the heat generated between the tool pin and workpiece[24].

The plasticized zone is constricted due to the sharp temperature gradient near the interface. The volume of plasticized material swept during each revolution is determined by process parameters and tool design and material. Similar to the temperature distribution, the flow process too is asymmetric on either side of the weld line. The advancing side shows a clear distinction of the nugget and is subjected to high plastic deformation due to the high strain rates[12].

1.8 FSP VS. CONVENTIONAL TECHNIQUES

Conventional manufacturing techniques for surface composites like PTA, laser cladding, thermal spray technique and laser melt particle injection involve liquid phase and melting of the particles[25]. Two major microstructural disadvantages due to this process are the cast microstructure of the composite layer and the formation of interfacial

reaction products at the particle–matrix interface. The chances of segregation of particles due to difference in densities of particles and melt are high in these processes. Being a fusion state process, the layer is prone to contamination by gasses and the processes involve high heat input thus consuming a lot of energy.

FSP, on the other hand, is a solid state process involving low heat inputs and short thermal cycle. It gives better microstructural properties as compared to the traditional techniques due to grain refinement during the process. It also provides a better operational range along with selective processing. It also cuts down on the cost factor due to low consumption of energy (consuming only 2.5% of the energy needed for laser weld[13]). Hence, FSP has become an attractive tool to be used for the fabrication of surface composites.

1.9 OBJECTIVES AND JUSTIFICATION OF PROBLEM

Previously, friction stir welding has been used to weld 20 vol% Al_2O_3 reinforced AA2014 aluminum matrix composites (MMC) with monolithic AA2014 aluminum alloy[26]. Fernandez and Murr have studied the weld optimization of FSW of 20 vol% SiC reinforced A359 alloy and the behavior of the tool wear during the weld[27].

However, the application of FSP alone as a tool to fabricate surface composites is relatively new. Mishra et al.[28] discussed FSP as a novel fabrication technique for surface composites by producing a SiC (0.7 μm) – 5083Al composite layer. They showed that the bonding between the composite layer was affected by the tool traverse speed and the incorporation of SiC particles was dependent on the plunge depth of the tool during processing.

Lee et al.[29] have fabricated 5 – 10% nano - sized SiO_2 into AZ61 alloy matrix and studied the variation of hardness and superplasticity of the bulk composite. Morisada et al.[30] have reported fabrication of SiC_p (1 μm) – AZ31 along with microstructure and hardness study. Other work has been reported on Al1100 – NiTi[31], Fullerene – A5083[32] and SiC_p – Al[33] alloys in recent years. Limited work has been done to obtain a novel

methodology to fabricate surface composites. Literature on the effect of patterns milled for incorporating powder and the flow of particles has not been reported. The present work focuses on methods to incorporate SiC particles into the A11100 matrix and study the distribution and flow of the particles in the nugget region. A subsequent study on microstructural features and mechanical behavior has also been done.

1.10 BIBLIOGRAPHY

[1] D.D.L. Chung Composite Materials: Science and Applications Functional Materials for Modern Technnologies.

[2] N. Chawla, K.K. Chawla, Metal Matrix Composites, Springer 2006, 2 - 4.

[3] www.pirun.ku.ac.th/~b4555045/pdf/(5)Composite%20Material.ppt.

[4] http://www.uofaweb.ualberta.ca/mece/pdfs/Chapter1-06.pdf.

[5] http://www.ms.ornl.gov/programs/energyeff/cfcc/iof/chap24-6.pdf.

[6] R. Singh and J. Fitz-Gerald, J. Mater. Res., Vol. 12, No. 3, Mar 1997, 769 - 773.

[7] R. L. Deuis, J. M. Yellup & C. Subramanian, Metal-matrix composite coatings by PTA surfacing, Composites Science and Technology Vol. 58, 1998, 299-309.

[8] R. Tiwari, H. Herman, S. Sampath and B. Gudmundsson, Plasma spray consolidation of high temperature composites. Mater. Sci. Eng., 1991, A144, 127-131.

[9] J.H. Abboud and D.R.F. West, Ceramic-metal composites produced by laser surface treatment, J. Mater. Sci. Technol., 1989, Vol. 5, 725-728.

[10] G.E. Totten and H. Liang, Surface modification and mechanisms: friction, stress and reaction engineering, CRC Press, 2004, 617 - 619.

[11] A.B. Kloosterman, B.J. Kooi and J.Th.M.De. Hosson, Electron microscopy of reaction layers between SiC and Ti-6AL-4V after laser embedding, Acta Mater. Vol. 46, No. 17, 1998, 6205-6217.

[12] R.S.Mishra, M.W. Mahoney, Friction Stir Welding and Processing, ASM International, March 2007.

[13] R.S. Mishra and Z.Y. Ma, Friction stir welding and processing, Materials Science and Engineering, R Vol. 50, 2005, 1–78.

[14] R.S. Mishra and M.W. Mahoney, Friction stir processing: A new grain refinement technique to achieve high strain rate superplasticity in commercial alloys, Mater. Sci. Forum, Vol. 357-359, 2001, 507-514.

[15] H.G. Salem, A.P. Reynolds and J.S. Lyons, Scripta Materialia, Vol. 46, 2002, 337–342.

[16] Z.Y.Ma, R.S. Mishra, M.W. Mahoney and R. Grimes, Mater. Sci. Eng. A., Vol. 351, 2003, p 148.

[17] I. Charit and R.S. Mishra, Mater. Sci. Eng. A., Vol. 359, 2003, p 290.

[18] I. Charit, R.S. Mishra and M.W. Mahoney, Scripta Materialia, Vol. 47, 2002, p 631.

[19] I. Charit, Z.Y. Ma and R.S. Mishra, Hot Deformation of Aluminum Alloys III, Z.Jin, A.Beaudoin, T.R. Bieler and B.Radhakrishnan, Ed., TMS, 2003, 331 - 342.

[20] Z.Y. Ma, S.R. Sharma and R.S. Mishra, Metall, Mater. Trans A, Vol. 37A, 2006, p 3323.

[21] Z.Y. Ma, S.R. Sharma and R.S. Mishra, Scripta Materialia Vol. 54, 2006, p 1623.

[22] S.P. Lynch, D. Edwards, A. Majumdar, S. Moutsos and M.W. Mahoney, Friction Stir Processing of a High-Damping Mn-Cu Alloy Used for Marine Propellers, THERMEC 2003, Trans Tech Publications.

[23] W. Tang, X. Guo, J.C. McClure, L.E. Murr and A. Nunes, Heat input and temperature distibution in friction stir welding, J. Mater. Process. Manuf. Sci., Vol. 7, Oct 1998, 163-172.

[24] M.J. Russell and H.R. Shercliff, Analytical modeling of microstructure development in friction stir welding, Proc. First Int. Symp. on Friction Stir Welding, June 1999.

[25] J.D. Majumdar et al. , Compositionally graded SiC dispersed metal matrix composite coating on Al by laser surface engineering, Materials Science and Engineering A, Vol. 433, 2006, 241-250.

[26] J.A. Wert, Microstructures of friction stir weld joints between an aluminium-base metal matrix composite and a monolithic aluminium alloy, Scripta Materialia, Vol. 49, 2003, 607-612.

[27] G.J. Fernandez and L.E. Murr, Characterization of tool wear and weld optimization in the friction-stir welding of cast aluminum 359+20% SiC metal-matrix composite,

Materials Characterization, Vol. 52, 2004, 65-75.

[28] R.S. Mishra, Z.Y. Ma and I. Charit, Friction stir processing: a novel technique for fabrication of surface composite, Materials Science and Engineering, Vol. A341, 2003, 307-310.

[29] C.J. Lee, J.C. Huang and P.J. Hsieh, Mg based nano-composites fabricated by friction stir processing, Scripta Materialia, Vol. 54, 2006, 1415-1420.

[30] Y. Morisada, H. Fujii, T. Nagaoka and M. Fukusumi, Effect of friction stir processing with SiC particles on microstructure and hardness of AZ31, Materials Science and Engineering, A Vol. 433, 2006, 50-54.

[31] M. Dixit, J.W. Newkirk and R.S. Mishra, Properties of friction stir-processed Al 1100–NiTi composite, Scripta Materialia, Vol. 56, 2007, 541-544.

[32] Y. Morisada, H. Fujii, T. Nagaoka, K. Nogi and M. Fukusumi, Fullerene/A5083 composites fabricated by material flow during friction stir processing, Composites: Part A, Vol. 38, 2007, 2097–2101.

[33] W. Wang, Q. Shi, P. Liu, H. Li and T. Li, A novel way to produce bulk SiC_p reinforced aluminum metal matrix composites by friction stir processing, Journal of Materials Processing Technology, Vol. 209, 2009, 2099–2103.

I. STUDY OF VARIOUS PROCESS FEATURES FOR THE FABRICATION OF SURFACE COMPOSITES USING FRICTION STIR PROCESSING

B. Gattu and R.S. Mishra*

Center for Friction Stir Processing, Department of Materials Science and Engineering

Missouri University of Science and Technology, Rolla, MO 65409, USA

ABSTRACT

Friction stir processing was successfully used to fabricate a Al1100–SiC_p surface composite layer on Al1100 substrate. The effect of various process features on the distribution and flow of SiC_p was studied. The staggered and linear holes pattern used to fill the powder gave an optimum incorporation of SiC_p with minimal loss during the process. The loss of SiC_p during the processing was eliminated by using Al6016 thin sheet to cover the powder filled pattern. Improvement in distribution of SiC_p was obtained with the tool offset towards the retreating side from the center of the pattern. Multiple passes was found to improve the distribution of the SiC_p in the nugget along the longitudinal direction due to high deformation and inter-mixing.

Keywords: Friction stir processing; surface composites; Al-SiC_p; pattern; offset; direction; particle distribution; metal matrix composite.

* Corresponding author. Tel: +015733416361 Fax: +015733416934 E-mail: rsmishra@mst.edu

1.1 INTRODUCTION

Friction stir processing (FSP) is a modification of friction stir welding (FSW) which was invented at The Welding Institute (TWI) in 1991. It has been used as a tool to modify the microstructure of alloys to improve the superplastic behavior[1-6], to refine the cast structure of alloys[7-8] and to improve the corrosion resistance[9]. In this process, a non consumable rotating tool consisting of a specially designed pin and shoulder is driven into the base alloy and then made to traverse along a path where microstructural modification is required[10].

The idea of FSP as a tool to fabricate surface composites was first introduced by Mishra et al.[11] when they successfully fabricated a Al–SiC_p surface composite on an Al substrate. FSP, being a solid state process with low heat inputs and short thermal cycles, provides an edge over conventional surface composite manufacturing techniques such as cast sintering[12,13], plasma spray[14], laser cladding[15,16], laser melt particle-injection[17], PTA surfacing[18] and high energy electron beam irradiation[19,20]. These processes involve high processing temperatures and cause melting of the substrate and to some extent the reinforcing particles. This leads to formation of unexpected phases at the particle/matrix interface, which could change the fracture behavior, since the mechanical behavior and load transfer phenomena in the composites are influenced by the interfacial conditions. A great deal of accuracy is also required to control the microstructure evolution and to curb the defect formation during the processing.

Over the years, work has been reported on the fabrication of AZ31–SiO_2 [21], AZ31–SiC_p[22], Al1100–NiTi[23], A5083–Fullerene[24] and Al–SiC_p[25] using FSP. However, limited work has been reported on the study of methodology to incorporate the reinforcement into the substrate.

The focus of this work is to study various friction stir process features such as the patterns used to incorporate the powders, the offset of the runs and the direction of processing during multiple runs that can be employed to improve the distribution of the reinforcement in the matrix.

1.2 EXPERIMENTAL PROCEDURE

Patterns were drilled on Al1100 plates (6.6 mm thick) using a carbide tool of 2mm diameter in a mini–CNC machine. Schematics of different types of patterns and their geometrical specifications are provided in Figure 1.1 and Table 1.1, respectively. The objective was to obtain a surface composite of 2.0 mm depth on the Al1100 plates and accordingly, the depth of the holes which are contained by the patterns was selected as 1.8 mm.

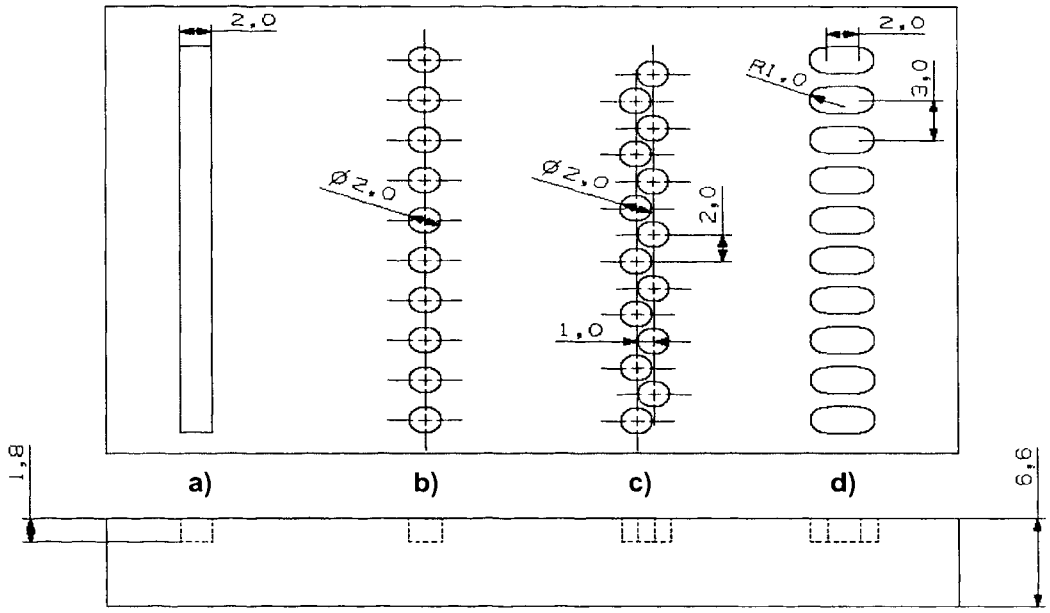

Figure 1.1. Schematics of the patterns used: a) Channel/groove, b) linear holes pattern, c) staggered pattern, d) gated pattern.

Table 1.1. Different patterns for powder incorporation and their features.

Pattern Name	**Diameter of Hole/Drill (mm)**	**Depth of Hole (mm)**	**Other Features**
Channel/Groove	2	1.8	--
Linear Holes	2	1.8	Distance between two holes = 3 mm.
Staggered Pattern	2	1.8	Distance between two holes = 4 mm. Distance between two rows = 1 mm.
Gated Pattern	2	1.8	Breadth of Gate= 2 mm. Distance between two consecutive gates = 2.5 mm.

Commercially obtained SiC powder (< 1500 grit) from Atlantic Equipment Engineers, was filled into the pattern (Figure 1.2). The particles were coarse and irregular

in shape and the average size was 5 μm - 7 μm. The SEM image in Fig 1.2 shows sharp edged features of the particles which is typical for the powders obtained by mechanical milling.

Figure 1.2. SEM image of SiC_p.

The dimensions and the images of the tools used for the study are provided in Table 1.2 and Figure 1.3. The criteria for selecting these tools were the depth of the hole and the targeted depth of surface composite layer. A221 tool was used to process open patterns (without any thin sheet as cover) and hence the pin length of 1.8 mm was selected corresponding to the depth of the hole.

In the experiments listed in section 1.2.2, a thin sheet of 1 mm thickness was used to cover the pattern. Hence, the tool A227 with a pin length of 2.98 mm was selected

(corresponding to sum of depth of hole and the thickness of the thin sheet). The diameter of the tool was selected corresponding to the width of the entire pattern, i.e. 3 mm. All the other features were kept similar to reduce the effect of the tool features while comparing the results.

Table 1.2. List of tools and their features.

Tool Name	Material	Tool Features	Pin Diameter (mm)	Pin Length (mm)	Shoulder Diameter (mm)	Shoulder feature
A221	Densimet	Conical Threaded	3	1.80	12.00	concave
A227	Densimet	Conical Threaded	2.97	2.98	14.90	concave

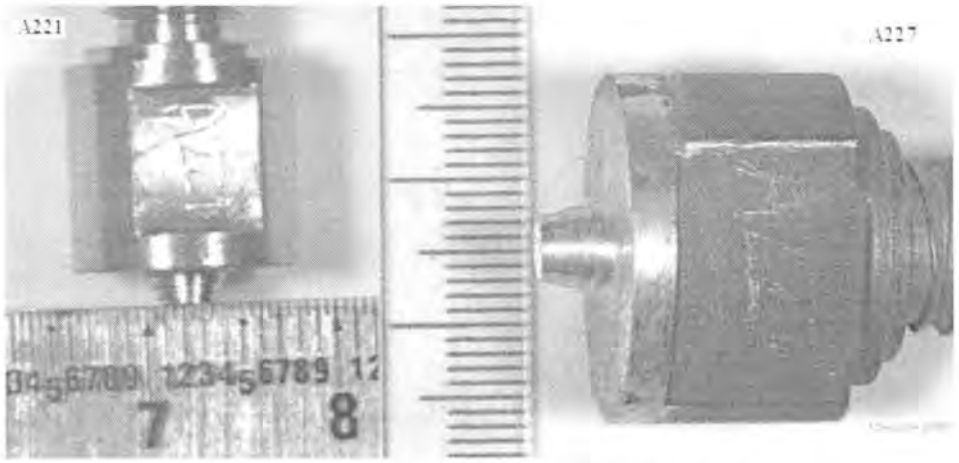

Figure 1.3. Images of the tool used in the study (scale shown in mm).

1.2.1 Effect of Pattern Geometry: FSP runs were made over the powder filled patterns (channel, linear holes, staggered and gated patterns) using the A221 tool with different parameters to optimize the quality of runs. SiC powder was filled into the drilled holes manually followed by tapping to make the powder settle down in the holes. This process was repeated until the holes were completely filled with powder. The process parameters were then fixed at 1000 rpm, 0.8467 mm/s (2 ipm), 2.5° traverse angle and a

plunge of 2.0 mm which provided the best results (least amount of flash, defect free surface and exit-hole analysis of FSP run). Fig 1.4 shows a visual image of the defective runs and the defect free run achieved by using the above parameters. Subsequently, the cross-section of the processed regions was analyzed on a macroscopic scale and the quality of the runs (based on visible observation during the processing described in section 1.3.1) was recorded for the four patterns. For the macroscopic analysis, images were taken across the nugget region using an optical microscope and then assembled to generate the macroscopic image.

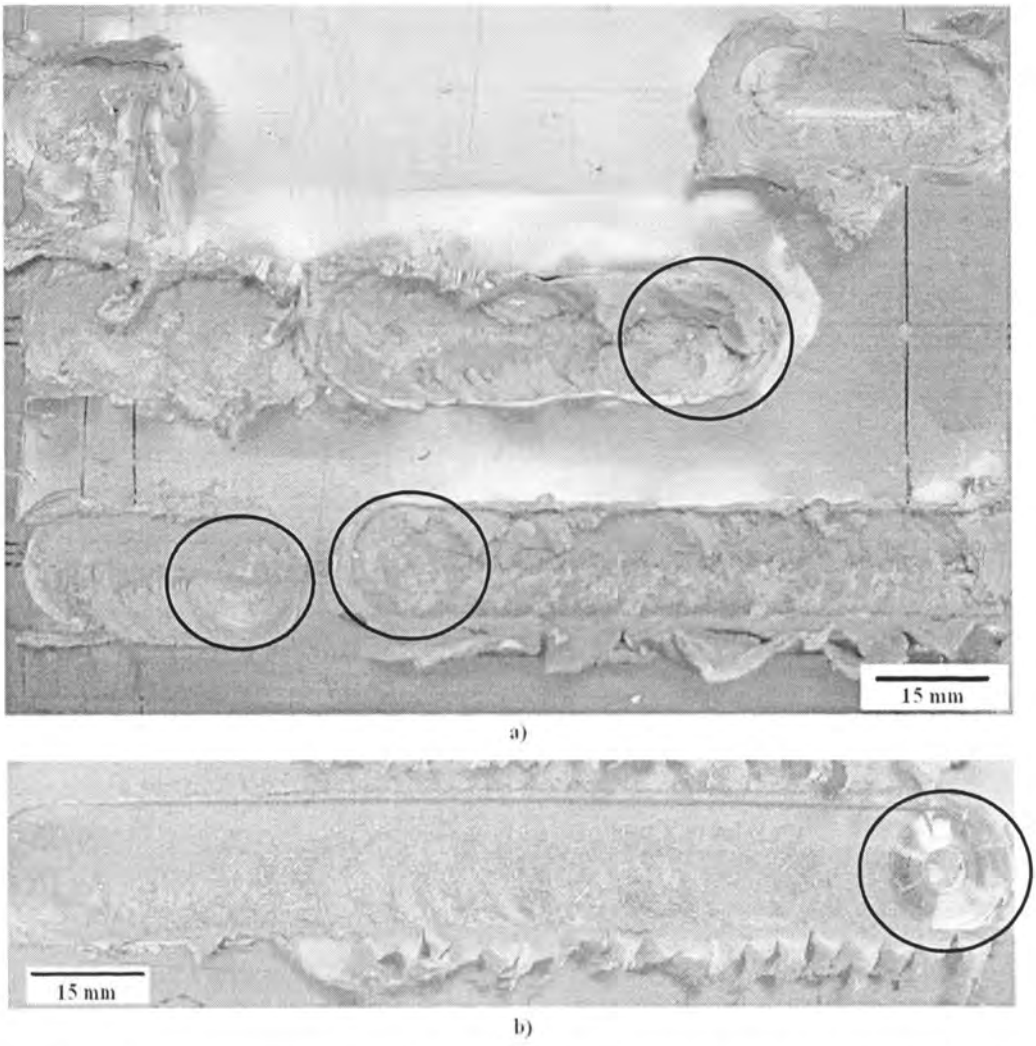

Figure 1.4. Study of process parameters. Image of a) defective runs and b) defect free run (exit holes marked by circles).

1.2.2 Effect of Offset and Thin Sheet Cover: Runs were performed using Al6016 sheet of 0.8 mm thickness to cover the linear holes pattern and without using the thin sheet as cover. To study the effect of offset three types of runs were made (Figure 1.5):

a. Offset towards advancing side.
b. No offset (center of the pattern).
c. Offset towards retreating side.

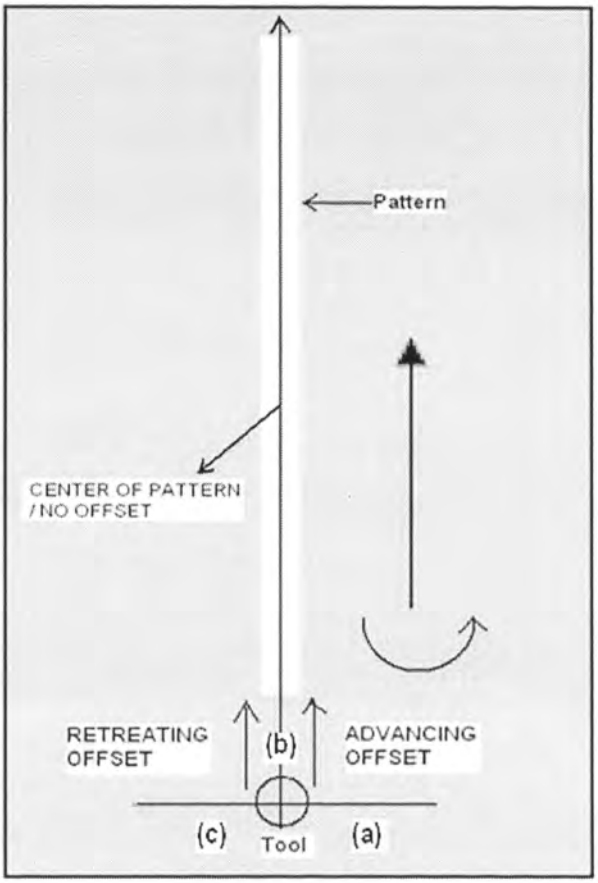

Figure 1.5. Pictorial representation of different types of offset for a pass.

The following runs were conducted using the A227 tool with 1000 rpm, 0.8467 mm/s (2 ipm), 2.5° traverse angle and a plunge of 3.1 mm as process parameters:

a) Run 1: 0.5 mm offset towards advancing side (open top)

b) Run 2: No offset (open top)

c) Run 3: 0.5 mm offset towards retreating side (open top)

d) Run 4: 0.5 mm offset towards advancing side with thin sheet cover

e) Run 5: No offset with thin sheet cover

f) Run 6: 0.5 mm offset towards retreating side with thin sheet cover

1.2.3 Direction vs. Offset of Multiple Pass and Linear Hole vs. Staggered Pattern: Linear holes and staggered holes pattern were chosen for further study according to the results of the experiments related to pattern geometry (section 1.2.1) which have been described in section 1.3.1. The following set of runs were conducted using the A227 tool with 1000 rpm, 0.8467 mm/s (2 ipm), 2.5° traverse angle and a plunge depth of 3.1 mm as process parameters to compare the effect of reversed direction with the effect of offset, during second pass and to compare the linear holes and staggered patterns:

a) Linear Hole Pattern:

   Pass 1: 0.5 mm offset towards retreating side.

   Pass 2: Reverse direction with 0.5 mm offset towards retreating side of the new run.

b) Linear Hole Pattern:

   Pass 1: 0.5 mm offset towards retreating side.

   Pass 2: 1.0 mm offset towards retreating side (from centre of pattern) in same direction.

c) Staggered Hole Pattern:

   Pass 1: No offset towards retreating side.

   Pass 2: 1.5 mm offset towards retreating side.

Subsequently, a macroscopic study of the longitudinal and transverse cross-sections of the nugget was conducted for all the experiments listed in this section.

1.3 RESULTS AND DISCUSSION

1.3.1 Effect of Pattern Geometry: The dimensions of the patterns and the depth of the holes can be varied depending on the geometry of the tool to achieve incorporation of the required amount of SiC_p and to obtain the required thickness of the composite layer. Hence, the approach of using powder filled patterns to incorporate the reinforcement provides flexibility in the fabrication of surface composite using FSP.

The linear channel pattern showed the least incorporation of the powder with heavy loss of powder. The rotation coupled with the tool tilt pushes the powder out of the groove ahead of the leading edge of the shoulder causing extreme loss of powder. Defect free runs with a significant amount of SiC_p incorporation and minimized powder loss were obtained for the linear and staggered holes pattern (Table 1.3 and Figure 1.6). Table 1.3 shows the recorded observations of the quality of runs such as powder loss during the process, defects in nugget, the observed powder incorporation and the distribution of particles in the nugget. The movement of the powder in these two patterns is restricted since it is pushed against the walls of the hole. This reduces the amount of powder pushed out of the pattern and thus, improves the process of powder–tool interaction.

Table 1.3. Recorded observations for the patterns.

Sr. No	Pattern	Powder loss	Defects	Powder Incorporation	Distribution
1	Channel /Groove	High	No defects	Very Low	Less uniform
2	Linear Holes	Less	No defects	Significant	More uniform
3	Staggered Pattern	Very Less	No defects	Significant	More uniform
4	Gated Pattern	Less	Large defects at the bottom of nugget	Significant	Less uniform

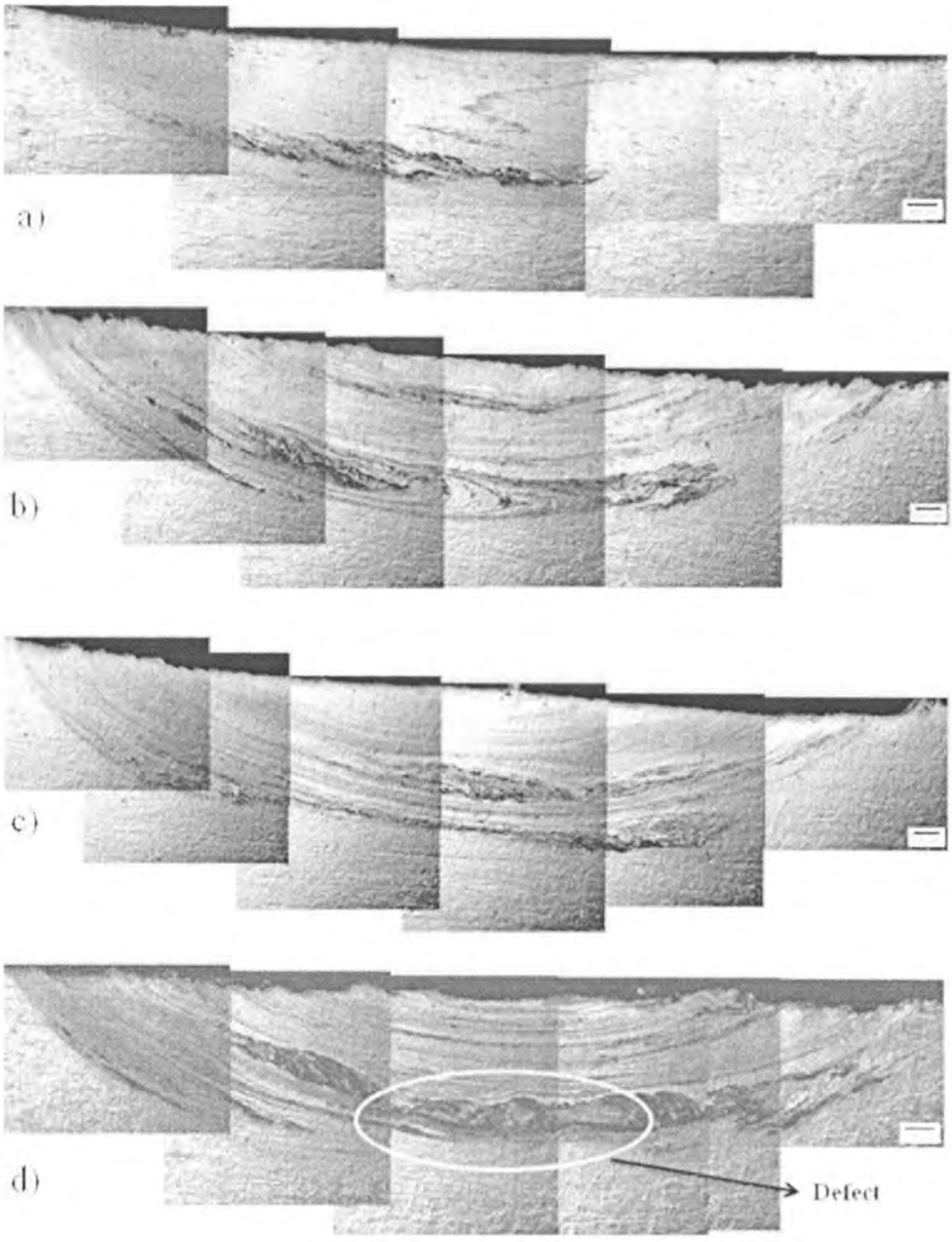

Figure 1.6. Nugget transverse cross-section for different patterns, a) channel/groove, b) linear holes c) staggered pattern, and d) gated pattern. Advancing side to left and retreating side to the right.

The gated channel had defects at the bottom of the nugget due to the insufficient availability of substrate material to fill the void region at that particular instance. Different amounts of powder loss were observed during the runs since the open patterns

provide a free route for the powder to escape and hence, the targeted powder incorporation could not be achieved. Except for the gated pattern, the runs showed good adhesion between the composite layer formed and the base material with few voids or porosity defects.

1.3.2 Effect of Offset and Thin Sheet Cover: Longitudinal (Figure 1.7) and transverse (Figure 1.8) cross-sections show that higher powder incorporation (or no loss of powder) is achieved by using the thin sheet as cover over the linear holes pattern when compared to the open linear hole pattern (without using thin sheet as cover) which showed a rough surface finish and higher loss of reinforcement during processing.

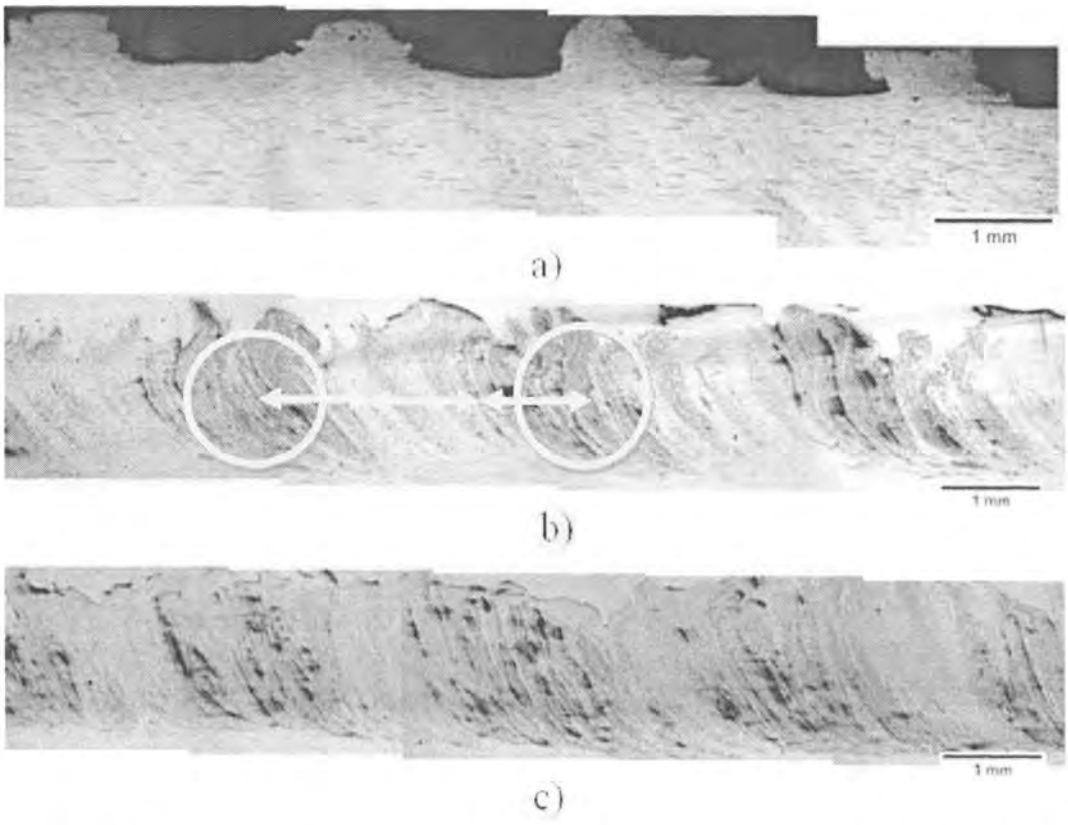

Figure 1.7. Longitudinal cross-section of a) open run with offset towards retreating side, b) thin sheet cover without offset, and c) thin cover sheet with offset towards retreating side (refer section 1.2.2 for process features of the runs). Marked circles explained in text.

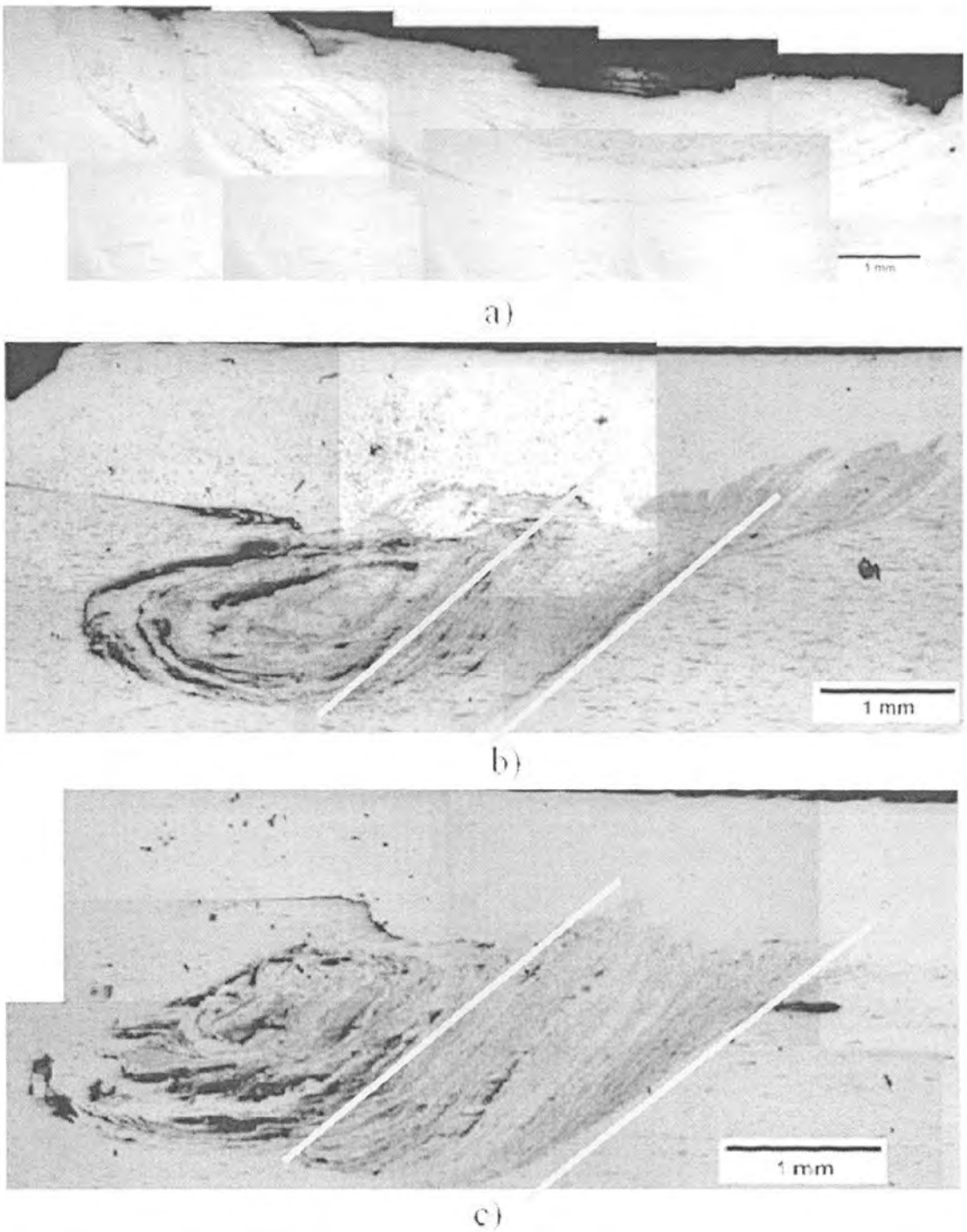

Figure 1.8. Transverse cross-section of a) open run with offset towards retreating, b) and c) thin sheet cover without offset and with offset towards retreating side, respectively (refer section 1.2.2 for process features of the runs).

The thin sheet used to cover the pattern, restricts the flow of the powder out of the pattern ahead of the tool. The powder is well distributed towards the advancing side while agglomeration takes place towards the retreating side. The material on the advancing side is subjected to high shear rates and hence, the particles move larger distances along with the Al1100 material.

The particle distribution along the longitudinal cross-section follows the periodicity of the pattern. The distance between the centers of two consecutive zones with high powder incorporation (marked by circles in Figure 1.7b) is 3 mm, which is the distance between two consecutive holes of a linear holes pattern. It is expected that, spacing the holes closer decreases the ratio of substrate material to SiC powder and gives defective runs due to insufficient availability of Al1100 material as can be observed in grooved and gated channel pattern which formed defective runs (Fig 1.6).

Better distribution of particles is obtained when the tool offset (line of traverse) is towards the retreating side since the tool encounters the major volume of the powder at the advancing side leading to better particle distribution. The area between the two parallel markers in Figure 1.8 b) and c), shows the region where the particles are distributed evenly at the advancing side of the run. One of the common features of the friction stir processed region is the banding of particles which was observed in longitudinal cross-section and on the advancing side of the transverse cross-section. For process parameters of 1000 rpm and 0.8467 mm/s (2 ipm), within the time taken for 1 complete revolution of the tool (0.001 min) the tool traverses 0.05 mm. This discontinuity in the tool movement and the deposition of the material leads to the banding as can be seen on the advancing side nugget profile of linear holes pattern shown in Figure 1.8 (b) and (c).

1.3.3 Direction vs. Offset of Multiple Pass and Linear Hole vs. Staggered Pattern: Reversing the direction of the second pass provides better mixing of particles along the direction of the run as compared to the second pass made in the same direction (Figure 1.9). The periodicity in particle distribution is disrupted by imparting heavy

mixing in the nugget region by using multiple passes. Another way to achieve this is by employing low traverse speeds along with high rotational speeds, however, with an increase in the amount of heat and temperatures achieved during the process. A higher fraction of SiC_p in the nugget is obtained by using a staggered pattern as compared to linear holes due to optimum ratio of substrate material to SiC_p (Figure 1.9 and Figure 1.10). Further, in the staggered pattern the distribution is improved both in the longitudinal and transverse cross-sections.

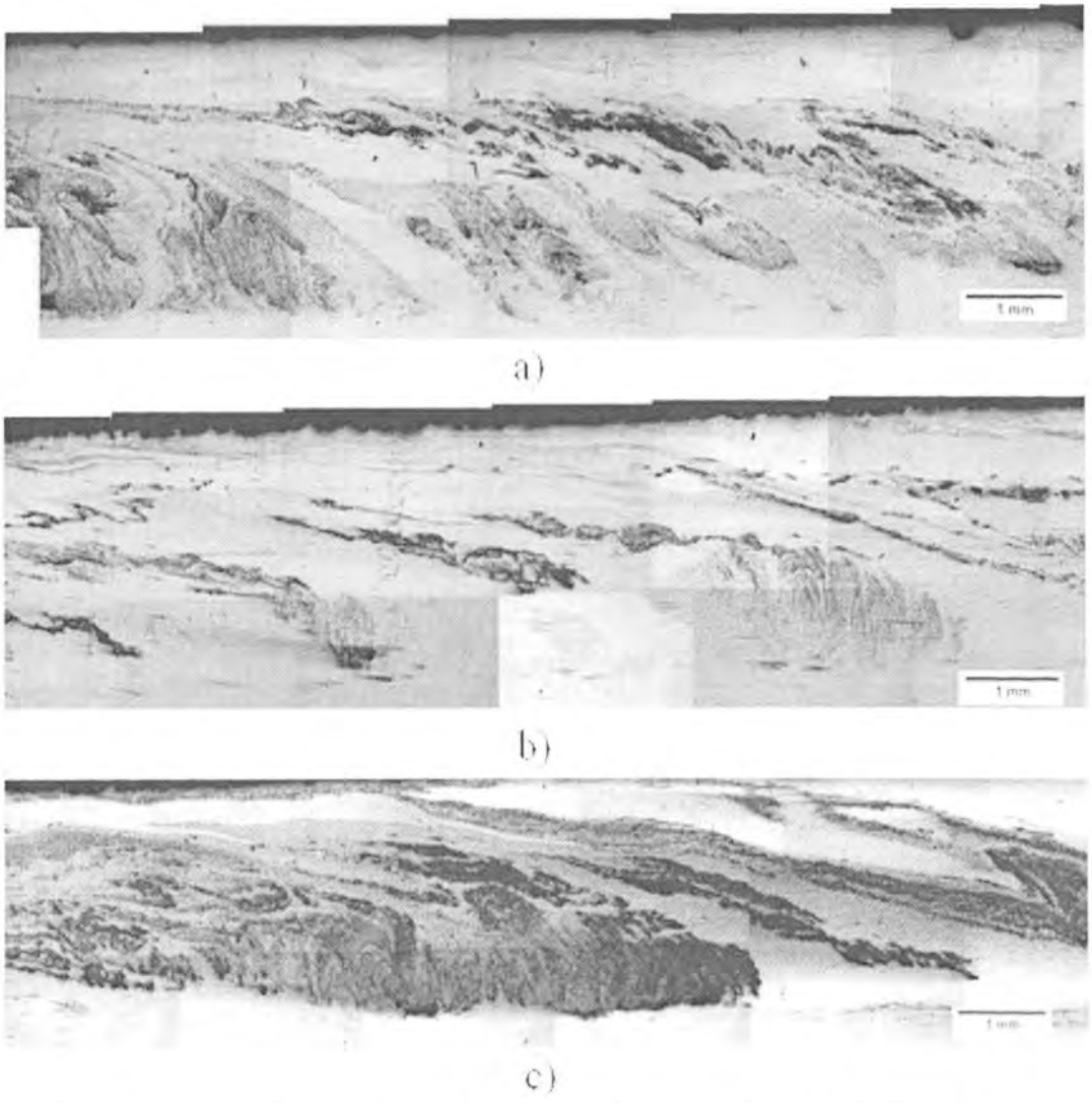

Figure 1.9. Longitudinal cross-section for multiple passes, a) pass 2 in reverse direction (linear holes), b) pass 2 in same direction (linear holes) c) staggered pattern with pass 2 done with an offset towards retreating side (refer section 1.2.3 for explanation).

A study of the transverse cross section of the nugget (Fig 1.10) shows that the composite layer adheres to the substrate and the interface shows no defects such as porosity due to insufficient flow of material both on the advancing and the retreating sides. The longitudinal cross-section also shows the same result. The powder flows towards the advancing side of the run when a multiple pass is employed. Thus, a staggered pattern closed with a thin sheet gives better results for fabricating surface composites as compared to the linear holes pattern.

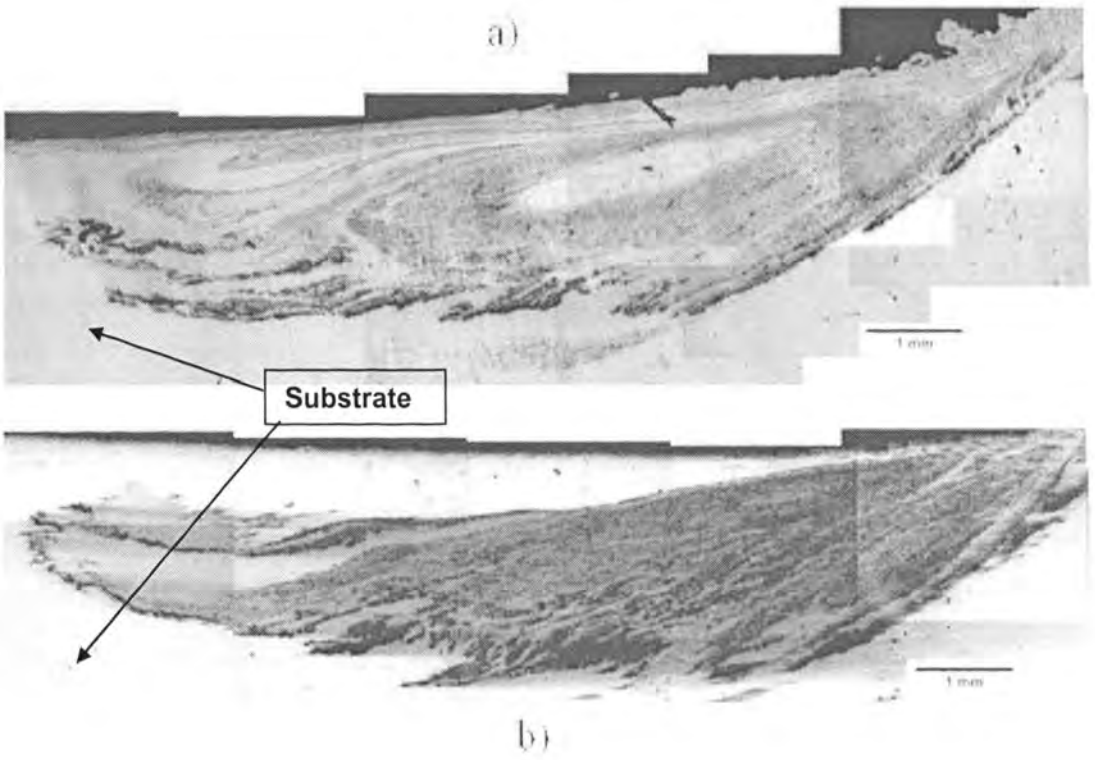

Figure 1.10. Transverse cross-section of multiple passes, a) linear holes pattern, and b) staggered pattern, with second pass done with an offset towards retreating side in the same direction(refer section 1.2.3 for definition of runs). Advancing side is to right.

1.4 CONCLUSIONS

A comparative study has been conducted to determine the response of the SiC particle distribution in the nugget to the patterns, offset of pass and direction of pass of

the FSP tool. A defect free Al1100 – SiC_p surface composite layer has been obtained with good bonding of the composite to the substrate.

Based on the experiments conducted, the following conclusions can be drawn:

1. Staggered patterns result in the highest incorporation of the SiC particles out of the four patterns used for filling the powder.
2. The loss of powder during FSP is avoided by the use of thin sheet as a cover over the pattern.
3. FSP carried out with an offset towards the retreating side with respect to the center of the pattern results in better particle distribution.
4. Multiple passes improve the distribution of SiC_p.
5. Reversing the direction of the second pass improves the distribution along the traverse direction.

1.5 ACKNOWLEDGMENTS

This work was performed under the NSF-IUCRC for Friction Stir Processing (NSF-EEC-0531019) and additional support of Boeing, PNNL, GM and Friction Stir Link for the Missouri S&T site is acknowledged.

1.6. REFERENCES

[1] R.S. Mishra and M.W. Mahoney, Mater. Sci. Forum, Vol. 357-359, 2001, 507-514.

[2] H.G. Salem, A.P. Reynolds and J.S. Lyons, Scripta Materialia, Vol. 46, 2002, 337–342.

[3] Z.Y. Ma, R.S. Mishra, M.W. Mahoney and R. Grimes, Mater. Sci. Eng. A., Vol. 351, 2003, p 148.

[4] I. Charit and R.S. Mishra, Mater. Sci. Eng. A., Vol. 359, 2003, p 290.

[5] I. Charit, R.S. Mishra and M.W. Mahoney, Scripta Materialia, Vol. 47, 2002, p 631.

[6] I. Charit, Z.Y. Ma and R.S. Mishra, Hot Deformation of Aluminum Alloys III, Z.Jin, A.Beaudoin, T.R. Bieler and B.Radhakrishnan, Ed., TMS, 2003, 331 - 342.

[7] Z.Y. Ma, S.R. Sharma and R.S. Mishra, Metall, Mater. Trans A, Vol. 37A, 2006, p 3323.

[8] Z.Y. Ma, S.R. Sharma and R.S. Mishra, Scripta Materialia, Vol. 54, 2006, p 1623.

[9] S.P. Lynch, D. Edwards, A. Majumdar, S. Moutsos and M.W. Mahoney, Friction Stir Processing of a High-Damping Mn-Cu Alloy USed for Marine Propellers, THERMEC 2003, Trans Tech Publications.

[10] R.S. Mishra and M.W. Mahoney, Friction Stir Welding and Processing, ASM International, March 2007.

[11] R.S. Mishra, Z.Y. Ma and I. Charit, Materials Science and Engineering, Vol. A341, 2003, 307-310.

[12] Y. Wang, X. Zhang, G. Zeng and F. Li, Mater. Des., Vol. 21, 2000, p 447.

[13] Y.S. Wang, X.Y. Zhang, G.T. Zeng and F.C. Li, Composites Part A, Vol. 32, 2001, p 281.

[14] M.C. Gui and S.B. Kang, Mater. Lett., Vol. 46, 2000, p 296.

[15] Y.T. Pei, J.H. Ouyang and T.C. Lei, Metall. Mater. Trans., Vol. 27A, 1996, 391-400.

[16] T.R. Tucker, A.H. Clauer, I.G. Wright and J.T. Stropki, Thin Solid Films, Vol. 118, Issue 1, 1984, 73-84.

[17] J.D. Ayers and T.R. Tucker, Thin Solid Films., Vol. 73, 1980, p 201.

[18] R. L. Deuis, J. M. Yellup and C. Subramanian, Metal-matrix composite coatings by pta surfacing, Composites Science and Technology, Vol. 58, 1998, 299-309.

[19] S.H. Choo, S. Lee and S.J. Kwon, Metall. Mater. Trans. A, Vol. 30A, 1999, p 1211.

[20] S.H. Choo, S. Lee and S.J. Kwon, Metall. Mater. Trans. A, Vol. 30A, 1999, p 3131.

[21] C.J. Lee, J.C. Huang and P.J. Hsieh, Scripta Materialia, Vol. 54, 2006, 1415-1420.

[22] Y. Morisada, H. Fujii, T. Nagaoka and M. Fukusumi, Materials Science and Engineering, Vol. A433, 2006, 50-54.

[23] M. Dixit, J.W. Newkirk and R.S. Mishra, Scripta Materialia, Vol. 56, 2007, 541-544.

[24] Y. Morisada, H. Fujii, T. Nagaoka, K. Nogi and M. Fukusumi, Composites: Part A, Vol. 38, 2007, 2097–2101

[25] W. Wang, Q. Shi, P. Liu, H. Li and T. Li, Jr. of Mat. Proc. Tech., Vol. 209, 2009, 2099-2103.

II. FABRICATION OF Al1100–SiC_p SURFACE COMPOSITES USING FRICTION STIR PROCESS AND STUDY OF THEIR MECHANICAL PROPERTIES

B. Gattu, R.S. Mishra*

Center for Friction Stir Processing, Department of Materials Science and Engineering, Missouri University of Science and Technology, Rolla, MO 65409, USA

ABSTRACT

Friction stir processing is successfully used to a fabricate Al1100–SiC_p surface composite on Al-1100 substrate. An increase in the number of overlapping passes shows improvement in the distribution of SiC_p in the matrix and the adhesion of the composite layer to substrate. The incorporation of SiC_p shows an increase in yield and ultimate tensile strengths. The matrix and matrix/SiC_p interface is free of porosity defects. The distribution of SiC_p varies from one region to another in the surface composite, however, the distribution is maintained over short distances within a given region.

Keywords: Friction stir processing; surface composites; Al-SiC_p; mechanical properties; particle distribution.

*Corresponding author. Tel: +015733416361, Fax: +015733416934, E-mail: rsmishra@mst.edu

2.1. INTRODUCTION

Metal matrix composites have found wide applications in aerospace, automotive and structural fields owing to their superior mechanical properties (high strength, elastic modulus and superplastic behavior) as compared to monolithic metallic alloys. In surface composites, the reinforcement exists only at the surface[1] thus, influencing the tribological properties (wear and erosion resistance, coefficient of friction, impact resistance) and the corrosion behavior of the composite material. The formation of mechanical and compositionally graded 3-D structures at the composite/substrate interface is one of the most important features of surface composites[2]. One of the

advantages of surface composites is that the surface alone can be tailored to get better tribological properties without sacrificing the properties of the bulk material.

Traditionally, cast sintering[3,4], plasma spray[5], laser cladding[6,7], laser melt particle-injection[8], PTA surfacing[9] and high energy electron beam irradiation[10,11] have been used for the fabrication of surface composites. These processes often involve high temperatures leading to the melting of the substrate material and in some cases melting of the injected particles[12]. Due to the presence of a liquid phase, high thermal input and high diffusion activity, byproducts are formed due to the reactions between the particle and alloy at the particle/matrix interface. The properties of the composites are strongly influenced by the conditions which exist at the particle/matrix interface and hence, the mechanical and corrosion response can be adversely affected.

Friction stir processing (FSP) originated from Friction Stir Welding (FSW) which was developed at The Welding Institute (TWI) in 1991. Previously, FSW was used to weld metal-matrix composite to monolithic alloys[13] and FSP was used to process composites manufactured by other processes[14]. Recently, friction stir processing has been used as a tool to fabricate surface composites. This idea was first introduced by Mishra et al.[15] in 2002. They successfully fabricated Al–SiC_p surface composites on Al substrate. Since then, FSP has been used to fabricate different combinations of surface composites[16-20]. In the present work, an effort has been made to study the effect of multiple passes on the distribution of SiC_p in the surface composite. Al1100-SiC_p surface composites were fabricated using friction stir processing and subsequently, a study of microstructure and mechanical properties of the surface composite was conducted.

2.2. EXPERIMENTAL PROCEDURES

The flowchart of the basic experimental procedure is shown in Figure 2.1. Patterns were drilled on Al1100 plates (6.6 mm thick) using a mini–CNC machine with a carbide tool of 2 mm diameter. Figure 2.2 and Table 2.1 provides the schematics and geometrical specifications of the patterns, respectively.

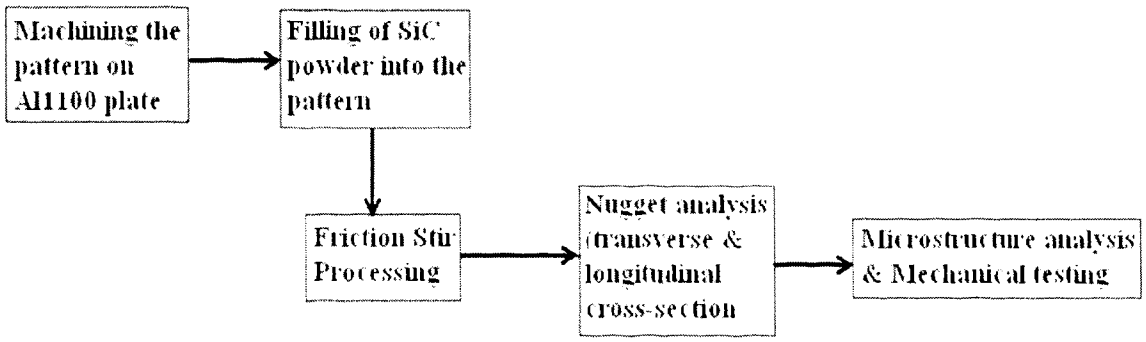

Figure 2.1. Flowchart showing sequence of the experimentation carried out.

Commercial SiC powder (< 1500 grit obtained from Atlantic Equipment Engineers) was filled into the pattern manually. Al6016 thin sheets (1 mm thick) were used to cover the pattern. The dimensions and the images of the tool used for the processing are provided in Table 2.2 and Figure 2.3a. The equipment used to perform FSP (Figure 2.3b) has one rotational (rotates around y – axis) and two translational degrees of freedom (traverses along x – axis and z – axis).

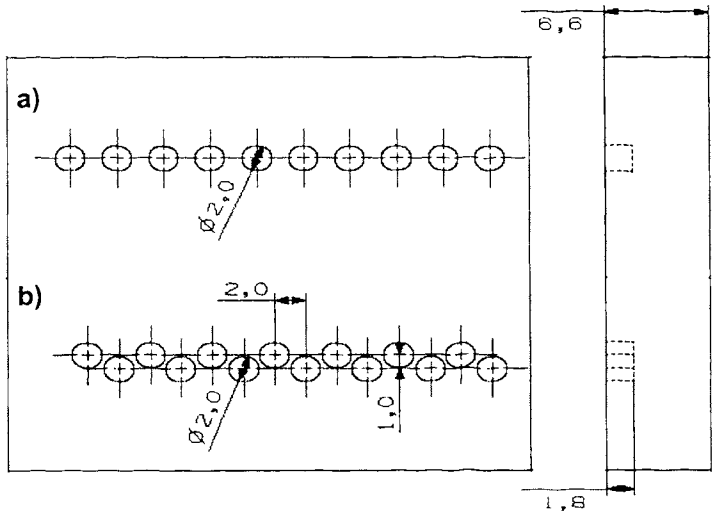

Figure 2.2. Schematics of the patterns used: a) linear holes pattern, b) staggered pattern.

Table 2.1. Different patterns for powder incorporation and their features.

Pattern Name	Diameter of Hole/Drill (mm)	Depth of Hole (mm)	Other Features
Linear Holes	2	1.8	Distance between two holes = 3 mm
Staggered Pattern	2	1.8	Distance between two holes = 4 mm Distance between two rows = 1 mm

The tool A227 was selected with a pin length of 2.98 mm to account for the depth of the holes drilled (1.8 mm) and the the thickness of the thin sheet (1 mm) used to cover the pattern. The width of the patterns drilled was 3 mm and hence, the diameter of the conical tool at the tapering end was selected in a way so that the region swept by the tool covers the entire width of the pattern. The tool was made out of Densimet, a tungsten alloy to withstand the forces generated on the tool during processing.

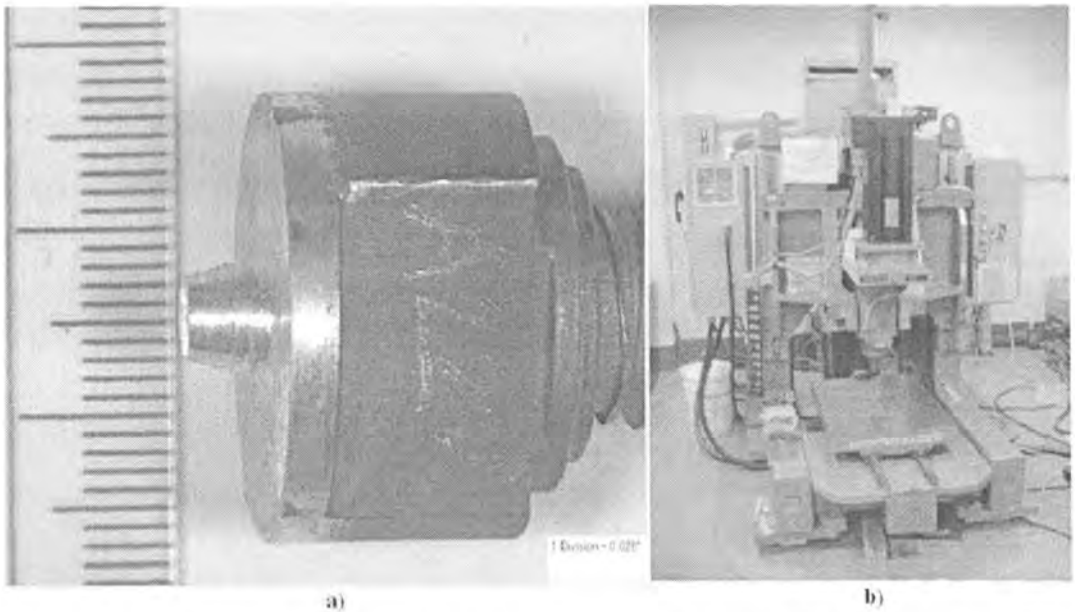

a) b)

Figure 2.3 a) Image of A227 tool (scale shown in mm) and b) friction stir processing machine.

Table 2.2. Tool used for FSP and its features.

Tool Name	Material	Tool Features	Pin Diameter (mm)	Pin Length (mm)	Shoulder Diameter (mm)	Shoulder feature
A227	Densimet	Conical Threaded	2.97	2.98	14.90	concave

Two sets of experiments were carried out as listed below.

Experimental Set 1:

The following set of experiments was conducted to study the effect of multiple passes with 100% overlap (rpm – revolutions per minute):

a. Staggered pattern 1:
   First pass: 1000 rpm, 0.8467 mm/s, 2.5° travel angle, 3.2 mm plunge depth.
   Second pass: 1000 rpm, 0.423mm/s, 2.5° travel angle, 3.2 mm plunge depth.
b. Staggered pattern 2:
   First pass: 1000 rpm, 0.8467 mm/s, 2.5° travel angle, 3.2 mm plunge depth.
   Second pass: 1000 rpm, 0.423 mm/s /2.5° travel angle, 3.5 mm plunge depth.
c. Staggered pattern 3:
   First pass: 1000 rpm, 0.8467 mm/s, 2.5° travel angle, 3.2 mm plunge depth.
   Second pass: 1000 rpm, 0.423 mm/s, 2.5° travel angle, 3.2 mm plunge depth.
   Third pass: 1000 rpm, 0.423 mm/s, 2.5° travel angle, 3.5 mm plunge depth.

A travel angle of 2.5° gives the necessary forging pressure on the material at rear of the tool shoulder during FSP and hence, helps in the consolidation of the material without the lift off of thin sheet due to the shoulder. Based on previous experiments the speed of rotation and traverse speed were selected as 1000 rpm and 0.8467 mm/s (or 2 inches per minute) respectively. The lift off of the thin sheet used to cover these patterns was avoided by employing these parameters when the thin sheet was held in position solely by the clamping mechanism.

In the subsequent passes, the traverse speed was decreased to impart heavy mixing by increasing the plastic flow of the material around the tool and the plunge depth was increased to provide downward forging pressure which is expected to improve the properties of the composite – substrate interface by reducing the FSP defects.

Experimental Set 2:

A second set of experiments was conducted with 1000 rpm, 0.8467 mm/s traverse speed, 2.5° traverse angle and a plunge depth of 3.1 mm as process parameters. In this set, the run centerline was offset with respect to the pattern centerline. This is in contrast to the experimental set 1 outlined earlier, where the centerline of the run matched with the centerline of holes pattern. The distance of offset is a fraction of the pin diameter (~3 mm).

a) Linear hole pattern:

   Pass 1: 0.5 mm offset towards retreating side.

   Pass 2: Reverse direction with 0.5 mm offset towards retreating side of the new run.

b) Linear hole pattern:

   Pass 1: 0.5 mm offset towards retreating side.

   Pass 2: 1.0 mm offset towards retreating side (from centre of pattern) in same direction.

c) Staggered hole pattern:

   Pass 1: No offset towards retreating side.

   Pass 2: 1.5 mm offset towards retreating side.

The transverse and longitudinal (along the traverse direction at the centre of nugget) cross-sections of the processed regions were investigated using an optical microscope. For the mechanical study, 1 mm of the processed surface was milled off corresponding to the thickness of thin sheet cover and mini-tensile specimens with thickness ranging from 0.6 - 0.8 mm (dimensions shown in Figure 2.4) were milled from the center of the nugget. Tensile tests were carried out at ambient temperature and at 1×10^{-3} s^{-1} nominal strain rate using a screw-driven mini-tensile machine.

An unreinforced run without SiC_p and with Al6016 sheet as cover over the substrate was made at 1000 rpm, 0.8467 mm/s traverse speed, 2.5 travel angle and 3.1 mm plunge depth. The tensile samples obtained from this run were used to compare with composite samples. The fracture surfaces of tested samples were observed using a scanning electron microscope.

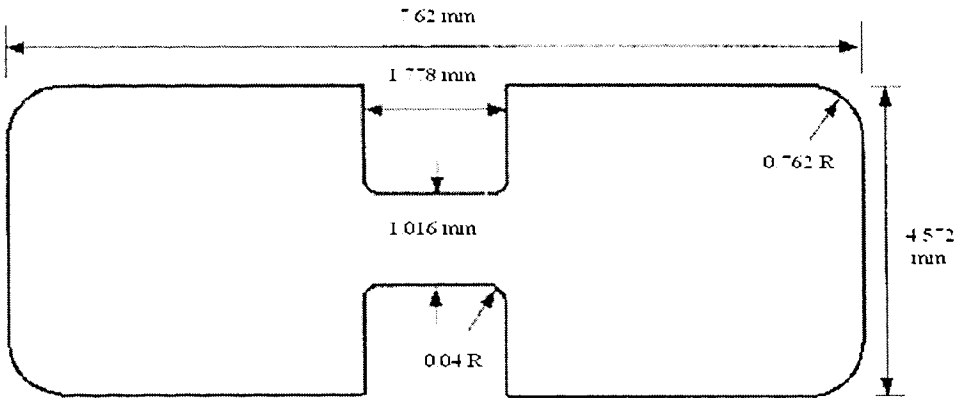

Figure 2.4. Dimensions of mini-tensile sample used for mechanical testing.

2.3. RESULTS AND DISCUSSION

2.3.1 Effect of multiple pass with 100% overlap: Increasing the number of passes over the pattern leads to improvement in the dispersion of SiC_p particles in the matrix. The transverse cross-sections (Figure 2.5) show a reduction in agglomeration and porosity and FSP defects as the number of passes increase and when the plunge depth is increased during the subsequent passes. The number of passes increases the volume of nugget and hence, the volume % of SiC_p in the composite layer decreases (Fig 2.5c).

The longitudinal cross-sections (Figure 2.6) of the runs conducted in the first experiment shows the distribution of SiC_p in Al1100. The first pass in a multiple run is targeted to incorporate the SiC_p in the Al1100 matrix and the subsequent passes are

designed to achieve better distribution of particles and to improve the adhesion of the composite layer to the substrate by decreasing the FSP defects and imparting heavy mixing. Exp 1 Run A and Exp 1 Run B involve processing the material in two passes with a difference in plunge depth during the second pass. The transverse cross-sections (Fig 2.5 a, b) show a decrease in the spread of agglomeration and defects. In Run A the agglomeration is spread on the advancing side of the run while it is restricted only to the retreating side in Run B. By employing a third pass (Exp 1 Run C) the agglomeration and FSP defects were completely avoided (Fig 2.5 c). This improves the adhesion of the composite layer to the substrate alloy due to reduction in SiC_p agglomeration.

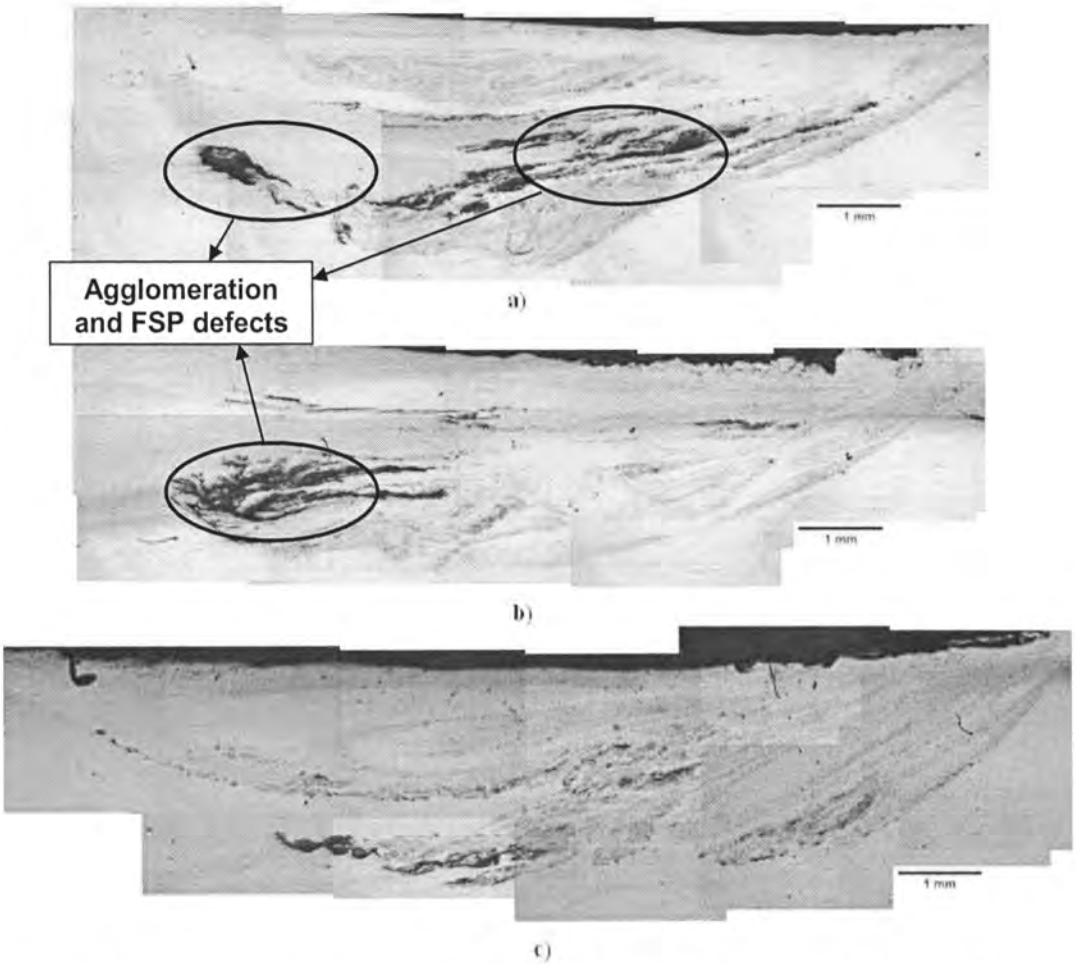

Figure 2.5. Transverse cross-section of a) Exp 1 Run A, b) Exp 1 Run B and c) Exp 1 Run C (advancing side to the right).

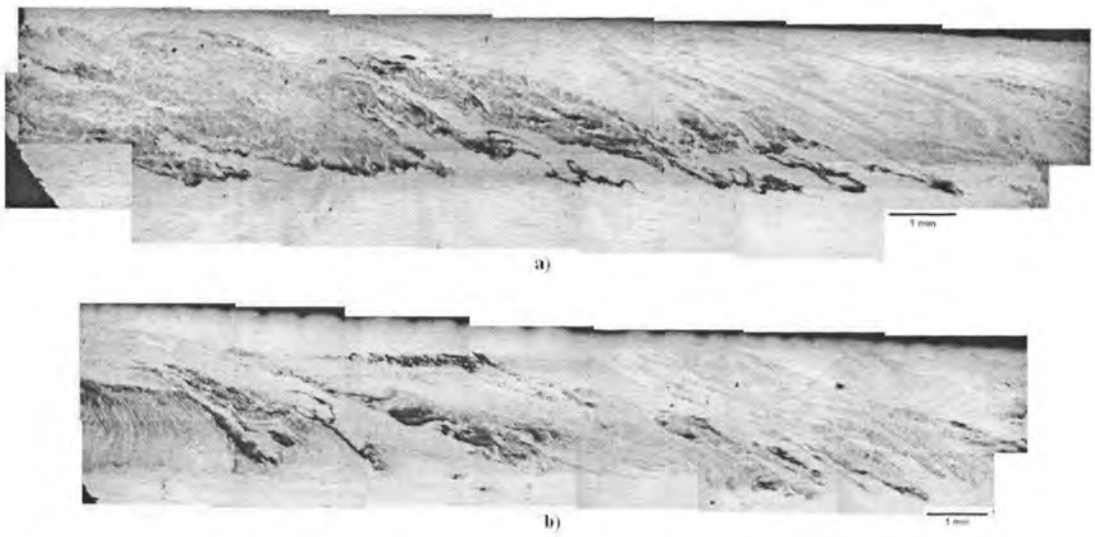

Figure 2.6. Longitudinal cross-section of a) Exp 1 Run A and b) Exp 1 Run B.

Efforts to replace Al6016 sheets with 1mm thin Al1100 sheets using a different combination of parameters (rotation speed ranging from 600–1000 rpm, traverse speed ranging from 0.2117 mm/s – 1.27 mm/s and plunge depth ranging from 3.1–3.4 mm) resulted in defective runs (Figure 2.7). Tearing of the thin sheets was observed due to the force applied by the shoulder during processing. This occurs due to lower strength of Al1100 sheet as compared to Al6016 sheet of the same thickness.

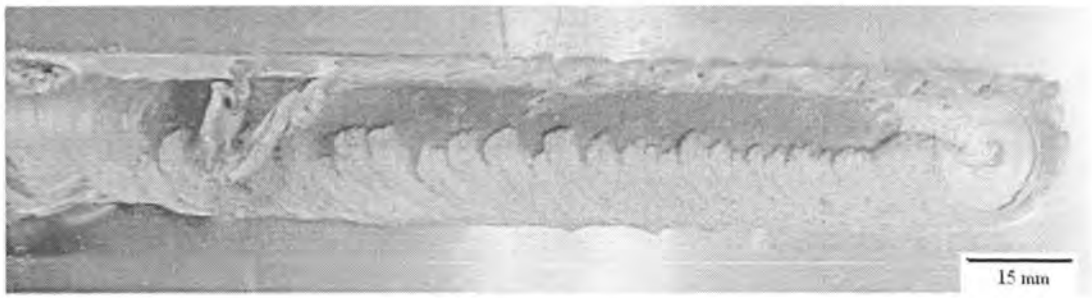

Figure 2.7. Image of the defective run produced with Al1100 thin sheet as cover.

2.3.2 Mechanical Properties: Tensile tests were carried out for the surface composite layer for each experiment (Exp 1 - Run A, Run B, Run C and Exp 2 - Run A, Run B, Run C) after milling off the top sheet. Three tensile specimens were cut from the center of the nugget and the results averaged for each experiment. The results vary over a wide range due to non uniformity in the SiC_p distribution.

Fig 2.8 shows the macroscopic image (taken from the top of the run) of the surface composite obtained in Exp 2 Run C after machining of 1 mm of the top surface to remove the sheet used to cover the pattern. It can be seen that the SiC powder (darker contrast) moves towards the advancing side of the nugget (indicated between the white markers) during the FSP run where SiC_p is continuous as compared to the retreating side.

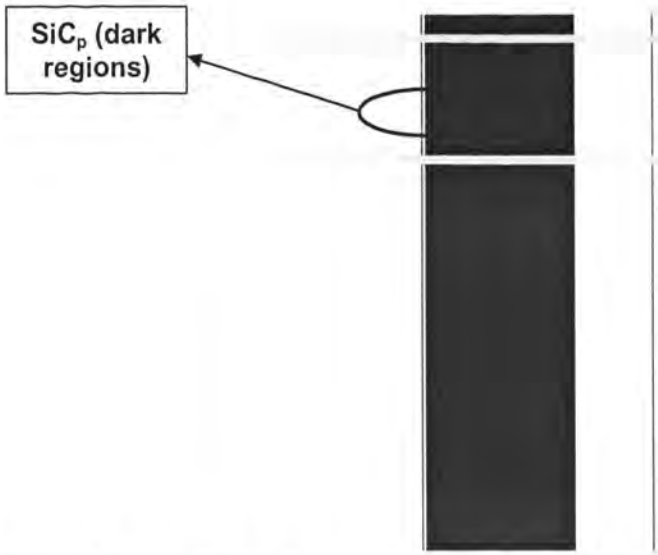

Figure 2.8. Image of the composite layer after milling 1 mm of the top surface (white markers show advancing side).

The processed material used for reference showed an average yield strength of 76.4 MPa, an ultimate tensile strength of 97.1 MPa and an elongation of 80.7%. Table 2.3 shows the mechanical properties of the surface composites obtained from the two sets of experiments.

Table 2.3. Mechanical properties of the surface composites.

Exp. No	Run	Average YS (in MPa)	Average UTS (in MPa)	Average % Elongation
1	A	110.4 ± 4.3	140.7 ± 10.0	31.1 ± 10.5
	B	95.7 ± 11.3	127.6 ± 20.6	43.3 ± 8.3
	B	124.6 ± 2.3	159.2 ± 1.0	42.2 ± 2.2
2	A	108.8 ± 3.9	142.5 ± 21.6	50.0 ± 15.0
	B	108.8 ± 4.1	145.4 ± 14.3	44.1 ± 0.8
	C	141.0 ± 0.5	176.9 ± 2.5	48.4 ± 2.8

The strength and ductility averaged over the three tensile tests conducted for each experiment are shown along with the standard deviation. The surface composite layer (obtained after machining the top sheet) showed higher yield strength and ultimate tensile strength as compared to the material processed without the SiC particles.

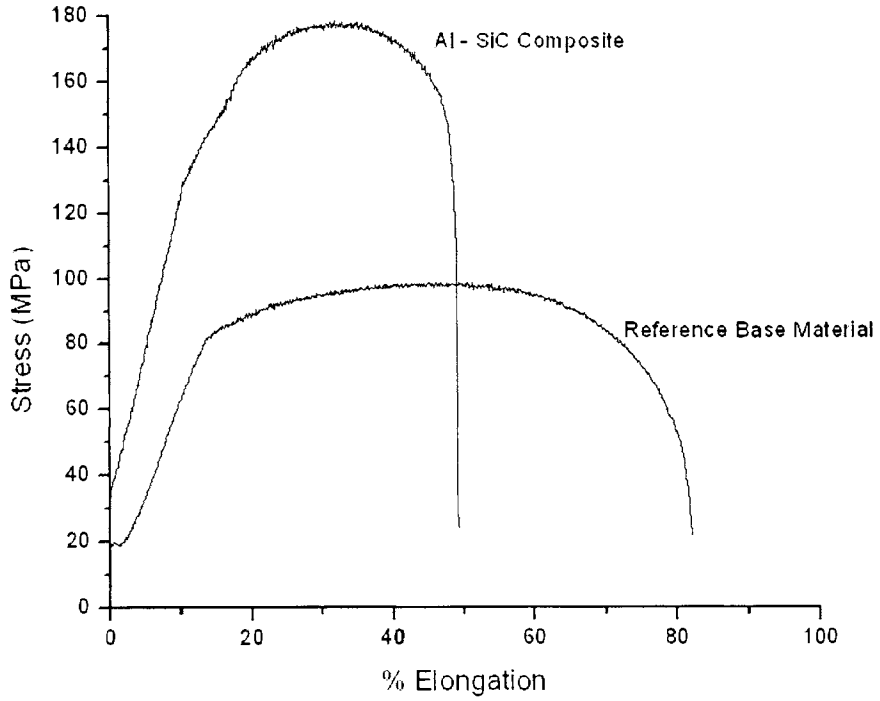

Figure 2.9. Mechanical behavior during tensile testing at ambient temperature and 1×10^{-3} s^{-1} strain rate.

Experiment 2 Run C showed the highest improvement of strength. The ductility of the surface composite for all conditions is lower as compared to that of the reference material. The surface composite fabricated by using a staggered pattern (Exp 2 Run C) showed better strength than that fabricated using the linear holes pattern (Exp 2 Run A and B). Figure 2.9 shows a comparison of the mechanical behavior of the surface composites (Exp 2 Run C) with respect to the reference material during the tensile test. The UTS and YS of the Al – SiC composite show an increase however, with a decrease in ductility. There is a significant variation in the plastic elongation of reference material and the surface composite layer. The SEM analysis of the fracture surface supported by tensile data showed ductile fracture behavior as indicated by the dimpled morphology in Figure 2.10.

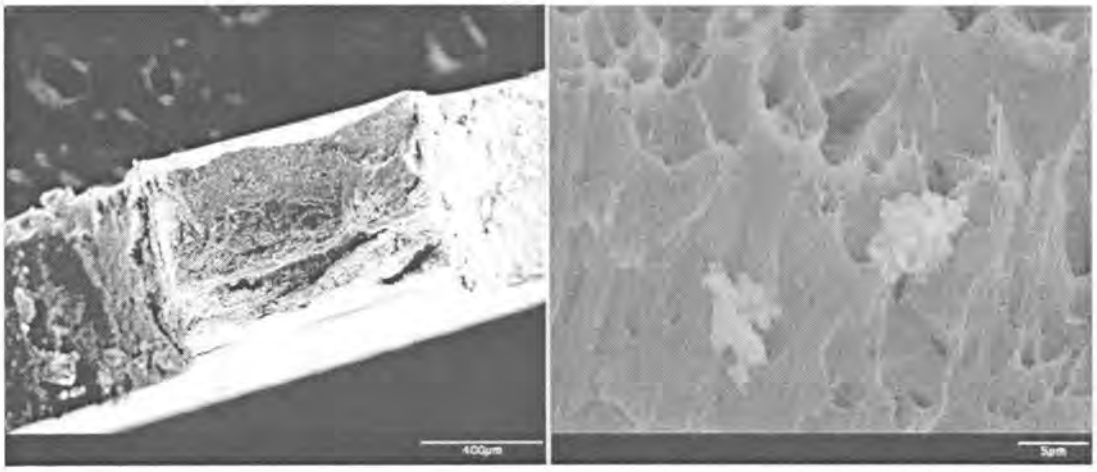

Figure 2.10. Typical SEM image of the fracture surface after tensile test of surface composite.

2.3.3 Microstructural analysis of surface composite: Microstructure (Figure 2.11, Figure 2.12 and Figure 2.13) of the surface composite fabricated in Exp 2 Run C (staggered pattern) showed SiC_p reinforced in a defect free Al1100 matrix. There is a diffused transition layer (shown using the white markers) between the surface composite and the substrate (Figure 2.11).

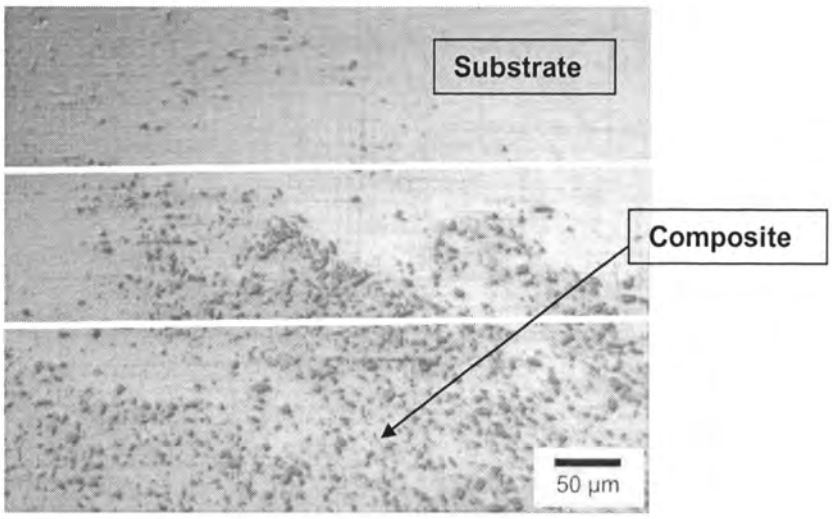

Figure 2.11 Surface composite/substrate interface.

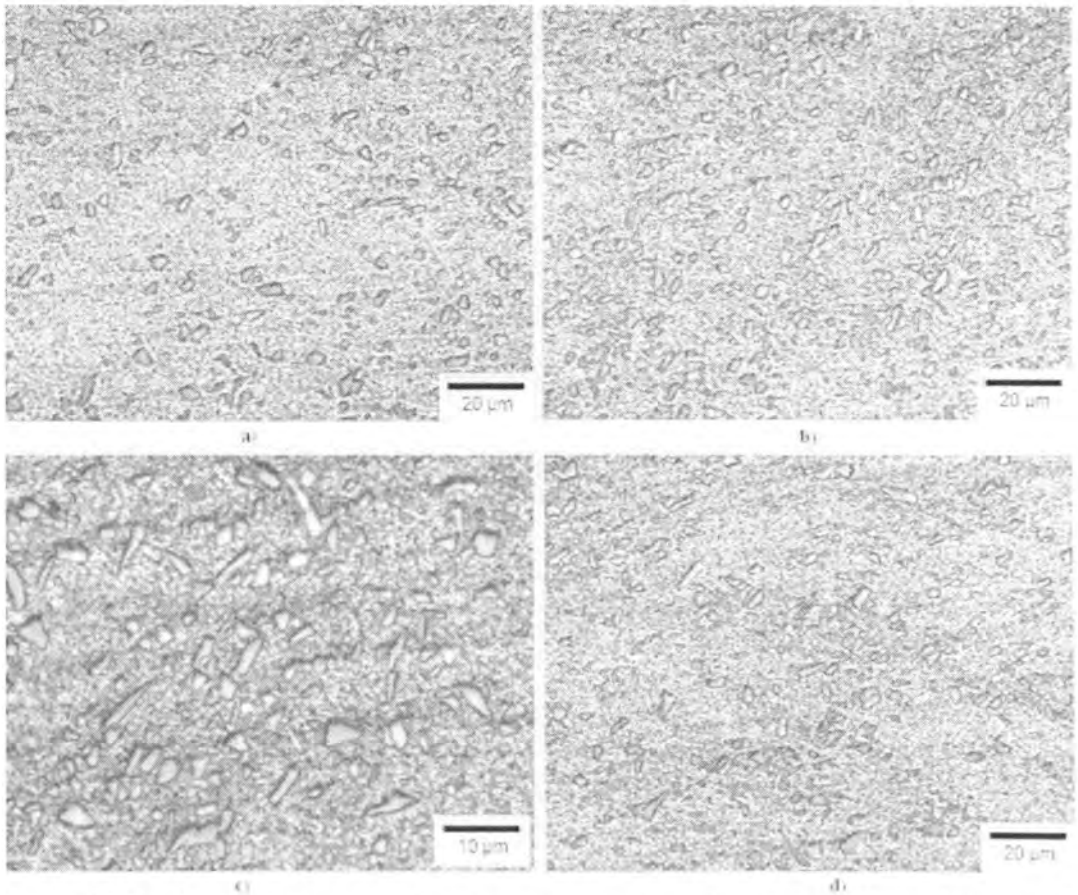

Figure 2.12. Microstructure in the transverse cross-section recorded at a) region A (advancing side), b) region B (advancing side), c) region A (higher magnification), and d) retreating side. (Exp 2 Run C)

This smooth transition layer is expected to reduce the interfacial stresses between the surface composite and substrate material improving the performance in potential structural applications. The distribution of SiC_p varied from one region to another as can be seen from Figure 2.12a and Figure 2.12b which were taken at different places on the advancing side. Region A shows lower volume fraction of SiC_p as compared to Region B. However, within a given region (A or B) the even distribution of SiC_p was maintained. The same behavior is seen in the longitudinal cross section of the nugget (Figure 2.13). The three distinct regions selected randomly, showed different volume fractions of SiC_p.

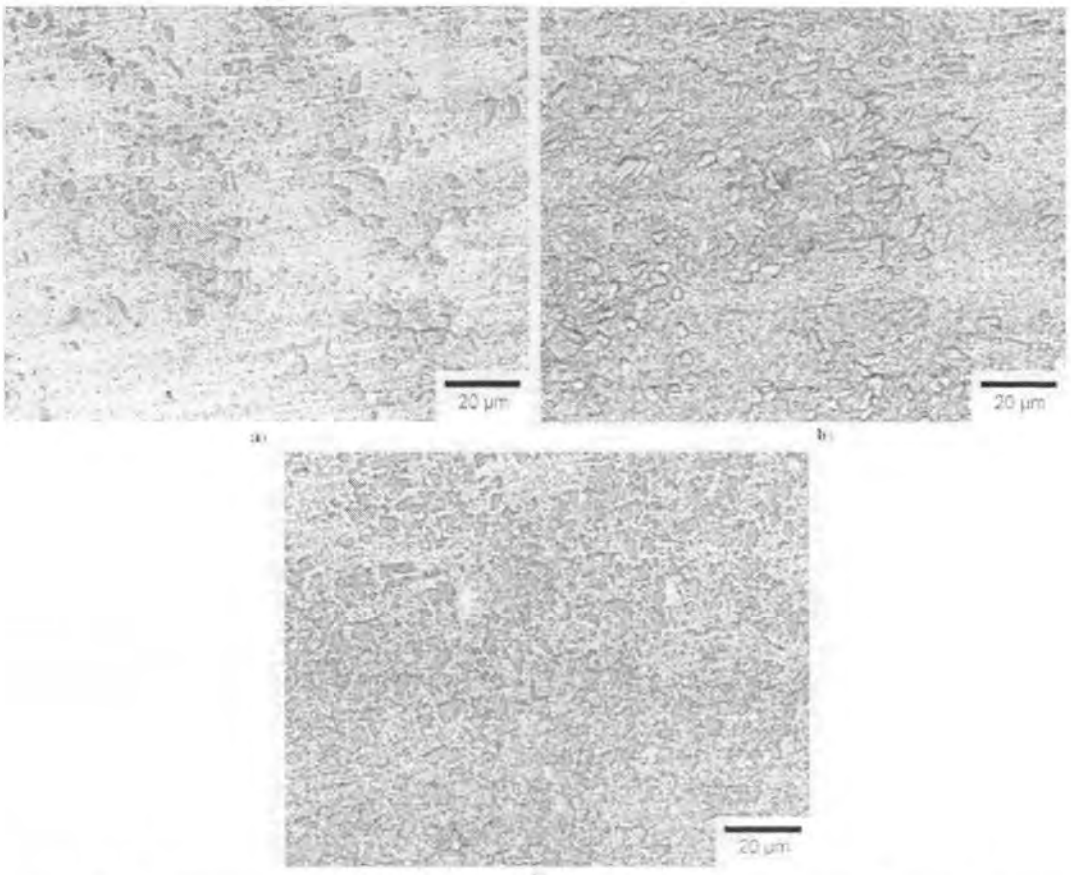

Figure 2.13. Microstructure in the longitudinal cross-section recorded at three different regions. (Exp 2 Run C)

2.4. CONCLUSIONS

Al1100–SiC_p surface composite was obtained on Al-1100 substrate using six different friction stir processing conditions and features.

1. The distribution of SiC_p in the matrix and adhesion of the composite layer to substrate were improved by employing multiple passes.
2. Al1100–SiC_p composite showed higher yield and ultimate tensile strengths than friction stir processed substrate material.
3. The composite layer showed ductile fracture under tensile loading.
4. Al1100 matrix and the matrix/SiC_p interface in the surface composite layer were free of porosity.
5. The distribution of SiC_p varied from one region to another.

2.5. ACKNOWLEDGMENTS

This work was performed under the NSF-IUCRC for Friction Stir Processing (NSF-EEC-0531019) and the additional support of Boeing, PNNL, GM and Friction Stir Link for the Missouri S&T site is acknowledged.

2.6 REFERENCES

[1] R. Singh and J. Fitz-Gerald, J. Mater. Res., Vol. 12, No. 3, Mar 1997, 769-773.

[2] T. Hirano, J. Teraki, and T. Yamada, in Proc. 1st Int. Symp. on FGM, edited by M. Yamanouchi, M. Koizumi, T. Hirai, and I. Shiota, Tokyo, Japan, 1995, p 5.

[3] Y. Wang, X. Zhang, G. Zeng, F. Li, Mater. Des., Vol. 21, 2000, 447.

[4] Y.S. Wang, X.Y. Zhang, G.T. Zeng, F.C. Li, Composites Part A, Vol. 32, 2001, p 281.

[5] M.C. Gui, S.B. Kang, Mater. Lett., Vol. 46, 2000, p 296.

[6] Y.T. Pei, J.H. Ouyang, T.C. Lei, Metall. Mater. Trans., Vol. 27A, 1996, 391–400.

[7] T.R. Tucker, A.H. Clauer, I.G. Wright, J.T. Stropk, Thin Solid Films, Vol. 118, Issue 1, 1984, 73-84.

[8] J.D. Ayers, TR. Tucker, Thin Solid Films., Vol. 73, 1980, p 201.

[9] R.L. Deuis, J.M. Yellup and C. Subramanian, Metal-matrix composite coatings by pta surfacing, Composites Science and Technology, Vol. 58, 1998, 299-309.

[10] S.H. Choo, S. Lee and S.J. Kwon, Metall. Mater. Trans. A, Vol. 30A, 1999, p 1211.

[11] S.H. Choo, S. Lee and S.J. Kwon, Metall. Mater. Trans. A, Vol. 30A, 1999, p 3131.

[12] J.D. Majumdar, B. Ramesh Chandra, A.K. Nath and I. Manna, Compositionally

graded SiC dispersed metal matrix composite coating on Al by laser surface engineering, Materials Science and Engineering, Vol. A433, 2006, 241-250.

[13] J.A. Wert, Microstructures of friction stir weld joints between an aluminium-base metal matrix composite and a monolithic aluminium alloy, Scripta Materialia, Vol. 49, 2003, 607-612.

[14] G.J. Fernandez and L.E. Murr, Characterization of tool wear and weld optimization in the friction-stir welding of cast aluminum 359+20% SiC metal-matrix composite, Materials Characterization, Vol. 52, 2004, 65-75.

[15] R.S. Mishra, Z.Y. Ma and I. Charit, Friction stir processing: a novel technique for fabrication of surface composite, Materials Science and Engineering, Vol. A341, 2003, 307-310.

[16] C.J. Lee, J.C. Huang, P.J. Hsieh, Mg based nano-composites fabricated by friction stir processing, Scripta Materialia, Vol. 54, 2006, 1415-1420.

[17] Y. Morisada, H. Fujii, T. Nagaoka, M. Fukusumi, Effect of friction stir processing with SiC particles on microstructure and hardness of AZ31, Materials Science and Engineering, Vol. A433, 2006, 50-54.

[18] M. Dixit, J.W. Newkirk and R.S. Mishra, Properties of friction stir-processed Al 1100–NiTi composite, Scripta Materialia, Vol. 56, 2007, 541-544.

[19] Y. Morisada, H. Fujii, T. Nagaoka, K. Nogi and M. Fukusumi, Fullerene/A5083 composites fabricated by material flow during friction stir processing, Composites: Part A, Vol. 38, 2007, 2097-2101.

[20] W. Wang, Q. Shi, P. Liu, H. Li and T. Li, A novel way to produce bulk SiCp reinforced aluminum metal matrix composites by friction stir processing, Journal of Materials Processing Technology, Vol. 209, 2009, 2099-2103.

2. CONCLUSIONS AND RECOMMENDATIONS

2.1. CONCLUSIONS

A composite layer of Al1100-SiCp over Al1100 substrate is successfully fabricated. Different patterns (groove, linear holes, staggered holes and gated channel) to achieve incorporation of SiC_p were compared. Staggered patterns result in the highest incorporation of the SiC particles out of the four different patterns. Using the process map it is expected that the thickness of the surface composite layer can be manipulated by using tool with different pin features. The loss of powder during FSP was avoided by the use of Al6016 thin sheet as a cover over the powder filled pattern. FSP carried out with an offset towards the retreating side with respect to the center of the pattern results in improved particle distribution when compared to other offsets. Reversing the direction of the second pass improves the distribution along the traverse direction. Agglomeration of particles is usually observed towards the retreating side and the distribution is enhanced at the advancing side as compared to the retreating side.

The distribution of SiC_p in the matrix and adhesion of the composite layer to substrate is improved by employing multiple passes. Al1100–SiC_p composite shows higher yield and ultimate tensile strengths as compared to the friction stir processed substrate material with the same process parameters. The composite layer showed ductile fracture under tensile loading. Al1100 matrix was void of defects due to FSP and the microstructure showed defect free matrix/ SiC_p interface in the surface composite layer. The distribution and volume fraction of SiC_p varied from one region to another.

2.2. CONTRIBUTIONS

The purpose of this work was to develop a novel methodology to successfully fabricate surface composites using friction stir processing. The main contributions of this research on friction stir processing to obtain Al1100-SiC_p surface composite on Al1100 are listed below:

- Design of staggered pattern to incorporate the powder.
- Use of Al6016 thin cover sheet to avoid the loss of powder during the process.

In commercial applications, this thin sheet can be machined off during post processing.

- Response of powder flow and distribution to the offset and multiple pass has been investigated.
- The mechanical properties of the surface composite under tensile loading showed an improvement in yield and ultimate tensile strength.

A novel approach is developed by using thin sheet cover over the pattern to avoid the powder loss followed by FSP and then machining the required thickness of top surface to fabricate the surface composite. This process is suited for industrial fabrication since there is no powder loss and the thickness of the composite layer on the surface can be varied by employing different depth of the holes drilled into the pattern and using different pin lengths of the tool while processing. The design of the pattern and the tool features can be varied to obtain different levels of SiC_p incorporation in the surface composite layer with good reliability. Hence, this approach provides flexibility in the fabrication of surface composites and is suited for industry, however with further improvements in the process.

The work provides an insight of the effect of different patterns used to fill the powder, a feature which has hardly been investigated, previously. The response of the powder flow and distribution to different process features such as offset, multiple pass and use of thin sheet to cover the pattern has been studied. A basic level investigation of microstructural features and mechanical behavior of the surface aspect is done.

2.3. RECOMMENDATIONS FOR FUTURE WORK

Based on the experience gained in this research, the following recommendations for future work are suggested:

- Though efforts have been made to improve the distribution of SiC_p in the matrix, still there is a lot of scope to obtain a more uniform distribution. In the future, work can be done employing a combination of multiple passes with appropriate offset and reversal of direction to achieve better distribution of reinforcement.

- The study of friction stir processing on the particle and grain size distribution can be done. Plastic deformation is utilized for movement of the particles and the substrate material. Hence, this study would lead to relation between the pre- and post- processed size distribution of the particles and grains along with the influence of initial particle size on grain size of the matrix.
- The wear behavior of the surface composite should be studied to establish the contribution of composite layer on the surface to improve wear resistance of the bulk material.
- The fatigue behavior of the surface composite under bending with the composite layer under compression should be studied. The composite layer is expected to have good compressive behavior and take the bending load acting on the material thus increasing the fatigue life.
- SiC_p can be replaced by powders of functional materials. For example, barium titanate ($BaTiO_3$) powder, a piezoelectric material can be used and a study can be performed to find its influence on the mechanical properties. Subsequently, the mechanical and fatigue behavior of this surface composites should be studied. It is expected that the piezoelectric property produces localized heating effect around the particles and contributes to stress (or strain) relaxation. This would reflect in the fatigue life of the surface composite.

VITA

Bharat Gattu was born on May 21, 1985, in Visakhapatnam, India. He received his Bachelor of Engineering degree in Metallurgical & Materials Engineering from Indian Institute of Technology Roorkee, India, in June 2006. He came to USA in August 2007 for pursuing his Masters. In July 2009, he received his Master of Science degree in Material Science and Engineering from Missouri University of Science and Technology (formerly University of Missouri-Rolla).